NEOPLASIA
www.neoplasia.com

Volume 14 Number 12 December 2012 pp. 1153–1163 **1153**

CITED1 Expression in Liver Development and Hepatoblastoma[1,2]

Andrew J. Murphy*, Christian de Caestecker*, Janene Pierce*, Scott C. Boyle†, Gregory D. Ayers‡, Zhiguo Zhao‡, Jaime M. Libes*, Hernan Correa§, Teagan Walter¶, Stacey S. Huppert¶, Alan O. Perantoni#, Mark P. de Caestecker¶, and Harold N. Lovvorn III***

*Department of Pediatric Surgery, Vanderbilt University Medical Center, Nashville, TN; †Department of Developmental Biology, Washington University School of Medicine, St Louis, MO; ‡Center for Quantitative Sciences, Vanderbilt University Medical Center, Nashville, TN; §Department of Pediatric Pathology, Vanderbilt University Medical Center, Nashville, TN; ¶Department of Cell and Developmental Biology, Vanderbilt University Medical Center, Nashville, TN; #Cancer and Developmental Biology Laboratory, Center for Cancer Research, National Cancer Institute, Frederick, MD; **Department of Medicine, Vanderbilt University Medical Center, Nashville, TN

Abstract

Hepatoblastoma, the most common pediatric liver cancer, consists of epithelial mixed embryonal/fetal (EMEF) and pure fetal histologic subtypes, with the latter exhibiting a more favorable prognosis. Few embryonal histology markers that yield insight into the biologic basis for this prognostic discrepancy exist. CBP/P-300 interacting transactivator 1 (CITED1), a transcriptional co-activator, is expressed in the self-renewing nephron progenitor population of the developing kidney and broadly in its malignant analog, Wilms tumor (WT). In this current study, CITED1 expression is detected in mouse embryonic liver initially on post-coitum day 10.5 (e10.5), begins to taper by e14.5, and is undetectable in e18.5 and adult livers. CITED1 expression is detected in regenerating murine hepatocytes following liver injury by partial hepatectomy and 3,5-diethoxycarbonyl-1,4-dihydrocollidine. Importantly, while CITED1 is undetectable in normal human adult livers, 36 of 41 (87.8%) hepatoblastoma specimens express CITED1, where it is enriched in EMEF specimens compared to specimens of pure fetal histology. CITED1 overexpression in Hep293TT human hepatoblastoma cells induces cellular proliferation and upregulates the Wnt inhibitors *Kringle containing transmembrane protein 1* (*KREMEN1*) and *CXXC finger protein 4* (*CXXC4*). *CITED1* mRNA expression correlates with expression of *CXXC4* and *KREMEN1* in clinical hepatoblastoma specimens. These data show that CITED1 is expressed during a defined time course of liver development and is no longer expressed in the adult liver but is

Abbreviations: EMEF, epithelial mixed embryonal/fetal histologic subtype of hepatoblastoma; CITED1, CBP/P-300 interacting transactivator 1; COG, Children's Oncology Group; CXXC4, CXXC finger protein 4; DDC, 3,5-diethoxycarbonyl-1,4-dihydrocollidine; DKK1, Dickkopf-related protein 1; FBS, fetal bovine serum; KREMEN1, Kringle containing transmembrane protein 1; MTT assay, 3-(4,5-dimethylthiazol-2-yl)-2,5-diphenyltetrazolium bromide assay; PCNA, proliferating cell nuclear antigen; qRT-PCR, quantitative real-time–polymerase chain reaction; WT, Wilms tumor

Address all correspondence to: Andrew J. Murphy, MD, Vanderbilt Children's Hospital, 2200 Children's Way, Suite 7102, Doctor's Office Tower, Nashville, TN 37232-9780. E-mail: andrew.j.murphy@vanderbilt.edu

[1]This work was supported by the Section of Surgical Sciences and the Ingram Cancer Center of the Vanderbilt Medical Center, by the National Cancer Institute (NCI) grant 5T32CA106183-06A1 (A.J.M.), and by NCI grant 4R00CA135695-03 (H.N.L.). The authors have no conflicts of interest to disclose.

[2]This article refers to supplementary materials, which are designated by Tables W1 to W3 and Figure W1 and are available online at www.neoplasia.com.

Received 14 June 2012; Revised 16 October 2012; Accepted 19 October 2012

DOI 10.1593/neo.12958

upregulated in regenerating hepatocytes following liver injury. Moreover, as in WT, this embryonic marker is re-expressed in hepatoblastoma and correlates with embryonal histology. These findings identify CITED1 as a novel marker of hepatic progenitor cells that is re-expressed following liver injury and in embryonic liver tumors.

Neoplasia (2012) 14, 1153–1163

Introduction

Hepatoblastoma is the most common liver cancer of childhood and is the third most common pediatric intra-abdominal malignancy after neuroblastoma and Wilms tumor (WT), respectively [1]. A variety of hepatoblastoma histologic subtypes exist, with epithelial-type hepatoblastomas being the most common [1]. Epithelial-type hepatoblastomas are subdivided into either epithelial mixed embryonal/fetal (EMEF) tumors, which contain both embryonal and fetal elements, or pure fetal histology tumors, which contain disorganized cells resembling fetal hepatocytes alone [1]. Pure fetal histology tumors have a markedly improved prognosis relative to EMEF tumors; in fact, pure fetal histology hepatoblastomas often are treated by surgical resection alone and do not require the administration of cytotoxic chemotherapy, a necessity in the treatment of all other hepatoblastomas [2].

Like other embryonal tumors, hepatoblastoma is thought to arise from persistence of progenitor cells that escape terminal epithelial differentiation during organogenesis and remain beyond birth. These stem-like cells may undergo subsequent genetic insults that result in neoplastic transformation in the embryonal tumorigenic sequence [3]. In support of this progenitor cell hypothesis, hepatoblastomas have been shown to share both a molecular phenotype and electron micrographic features consistent with hepatic progenitor cells [4,5]. Moreover, components of the Wnt signaling pathway, which plays a complex, but critical, role in promoting embryonic liver development [6], are activated in a large proportion of hepatoblastomas. In fact, hepatoblastoma has the highest reported frequency of activating β-catenin mutations of any cancer [7,8]. These findings indicate that aberrant activation of a common signaling pathway required for normal liver development may also play a role in the pathogenesis of hepatoblastoma.

CBP/P-300 interacting transactivator 1 (CITED1) is a non-DNA binding transcriptional co-activator that along with expression of an additional transcription factor, SIX2, identifies the self-renewing portion of nephron progenitor cells in the metanephric mesenchyme of the developing kidney [9,10]. In the embryonic kidney, CITED1 is expressed only in these progenitor cells during the period of nephrogenesis and is downregulated as these cells undergo differentiation en route to forming mature nephrons [9]. The functional role of CITED1 in kidney development is uncertain because *CITED1* null mice do not display altered nephrogenesis [9]. However, previous experiments have shown that CITED1 inhibits Wnt4-dependent transcriptional responses [11]. Because Wnt/β-catenin signaling in the metanephric mesenchyme is a critical regulator of early nephron differentiation [12], it is possible therefore that CITED1 modifies canonical Wnt/β-catenin signaling in these nephron progenitor cells even though genetic studies using *CITED1* null mice indicate that its developmental role is functionally redundant [9].

WT is an embryonal tumor that is the most common kidney cancer of childhood and is thought to arise from arrested epithelial differentiation of embryonic kidney nephron progenitor cells [13,14]. Like hepatoblastoma, dysregulation of Wnt signaling and mutation of β-catenin have been implicated in the pathogenesis of WT [15,16]. In this malignant context, we have previously shown that while CITED1 expression is absent in the postnatal kidney, persistent expression of CITED1 is observed in a broad spectrum of WT [17,18]. Moreover, gain-of-function studies indicate that CITED1 enhances cellular proliferation in a putative embryonal tumor cell line and overexpression of a dominant-negative CITED1 construct perturbs embryonal tumor formation in a mouse xenograft model [17,19]. Taken together, these data suggest that CITED1 may play a role in Wilms or embryonal tumorigenesis and that these activities may relate to its ability to block Wnt/β-catenin progenitor cell differentiation in this context.

On the basis of these findings, and given the roles of Wnt signaling in normal liver development and hepatoblastoma, we hypothesized that CITED1 misexpression might also play a role in the pathogenesis of hepatoblastoma. In these studies, therefore, we have characterized for the first time expression of CITED1 in hepatic development and hepatoblastoma. We have shown that CITED1 is expressed in hepatoblasts early in development. CITED1 expression is lost in the adult liver but is strongly expressed in experimental and human hepatoblastoma and also during hepatic regeneration following various forms of hepatic injury. Although the functional role of CITED1 in liver development, hepatoblastoma, and liver regeneration remains to be established, in light of its role as a potential modulator of Wnt signaling and its association with embryonal tumorigenesis in the kidney, these studies suggest that persistent CITED1 expression plays a role in regulating and promoting hepatoblastoma.

Materials and Methods

CITED1^{LacZ} *Reporter Mouse*

Development of the *CITED1*^{LacZ} reporter mouse has been previously described [20]. For whole-mount staining for β-galactosidase activity, embryos were isolated in cold phosphate-buffered saline (PBS) and fixed in 0.2% glutaraldehyde in PBS with 2 mM $MgCl_2$ and 5 mM EGTA for 15 minutes. Fixed embryos were equilibrated in β-Gal wash [0.1 M phosphate buffer (pH 7.3) containing 2 mM $MgCl_2$, 5 mM EGTA, 0.02% NP-40, and 0.01% Na deoxycholate] and stained overnight at 37°C in β-Gal wash containing 1 mg/ml X-Gal and 5 mM potassium ferrocyanate and ferricyanate. Embryos were visualized using light microscopy. Timed pregnancies were counted with the morning of vaginal plug appearance as day 0.5.

Hepatoblastoma and Liver Injury Specimens

Forty-one human hepatoblastoma specimens were included in this analysis. A total of 19 paraffin-embedded and snap-frozen hepatoblastoma tissue specimens were obtained from the Children's Oncology

Group (COG). Of these COG specimens, 11 were EMEF histology, while 8 were of pure fetal histology. Clinical data were not available or provided from the COG to correlate with patient outcomes. Twenty-two formalin-fixed, paraffin-embedded specimens were available from our institutional repository. Of these 22 institutional specimens, 17 were EMEF histology and 5 were of pure fetal histology. These specimens were only available for immunohistochemistry.

Forty-three paraffin-embedded murine hepatoblastoma specimens, induced chemically from *N*-nitrosodiethylamine, 2,3,7,8-tetrachlorodibenzo-*p*-dioxin, were available for analysis [21]. To compare CITED1 reactivation in other injury models, we subjected adult murine livers to two-thirds partial hepatectomy or to exposure for 21 days of a diet containing 0.1% 3,5-diethoxycarbonyl-1,4-dihydrocollidine (DDC), as previously described [22]. DDC-fed mice were allowed 1 day of recovery following DDC treatment and were sacrificed, and livers were subsequently fixed in 10% formalin and paraffin-embedded for immunohistochemical analysis. Mice undergoing two-thirds partial hepatectomy were sacrificed at 3 and 7 days and livers were similarly prepared for immunohistochemical analysis. All animal husbandry and experiments were conducted in accordance with the standards of and prior approval from the Vanderbilt University Medical Center Institutional Review Board and Institutional Animal Care and Use Committee.

Immunohistochemistry and Immunofluorescence

All tissue samples were subjected to heat-induced antigen retrieval in 10 mM citrate buffer. These 5-μm sections were incubated in affinity-purified rabbit anti-CITED1 (1:50 dilution; Lab Vision Corp, Fremont, CA) antibody for 1 hour at room temperature. Goat anti-rabbit secondary antibody (1:200 dilution; Santa Cruz Biotechnology, Santa Cruz, CA) was applied to tissues at room temperature for 45 minutes. Tissues were visualized with either a Vectastain ABC Kit (Vector Laboratories, Burlingame, CA) or DAKO Envision Kit (DAKOCytomation, Carpinteria, CA). Immunohistochemistry was coded on an ordinal scale of expression intensity (e.g., 0 = absent, 1 = weak, 2 = strong). Counts of expression were compared overall, in the cytosol, and in the nucleus by an observer blinded to the tissue samples. Proliferating cell nuclear antigen (PCNA) immunostaining was performed similarly using a 1:1000 dilution of mouse anti-PCNA antibody (Santa Cruz).

For immunofluorescence experiments, tissues were similarly treated and quenched using hydrogen peroxide. Mouse fetal heart, kidney, and liver specimens were blocked using mouse-on-mouse block (Vector Laboratories) with 0.5% hydrogen peroxide for 1 hour at room temperature. Sections were then incubated in rabbit anti-CITED1 (1:100; Lab Vision Corp) with mouse-on-mouse block, 10% goat serum, and 0.5% hydrogen peroxide in PBS overnight at 4°C. Anti-mouse HRP (1:750 dilution; KPL, Gaithersburg, MD) was added for 40 minutes at room temperature. For visualization of CITED1, anti-rabbit DyLight 549 (1:600 dilution; Jackson ImmunoResearch, West Grove, PA) or fluorescein isothiocyanate–conjugated (1:100 dilution; Jackson ImmunoResearch) antibodies were added for 2 hours at room temperature. For ureteric bud staining, monoclonal mouse cytokeratin 8 - (Troma-1 antibody, 1:50 dilution; Developmental Studies Hybridoma Bank, Iowa City, IA) was used. TOPRO-3 or 4′,6-diamidino-2-phenylindole, dilactate (DAPI) were used for nuclear staining.

Western Blot Analysis, β-Catenin Sequencing, and Quantitative Real-time–Polymerase Chain Reaction

CITED1 Western blots were performed, as previously described [18]. Immunoblots were performed using affinity-purified rabbit anti-CITED1 (1:1000 dilution; Lab Vision Corp), M2 anti-FLAG antibody (1:1000 dilution; Sigma Chemical Co, St Louis, MO), and mouse anti–β-actin (1:5000 dilution; Sigma Chemical Co). Densitometry was performed using Photoshop (Adobe, San Jose, CA). β-Catenin Western blots were performed similarly using rabbit anti–β-catenin antibody (1:1000 dilution; Cell Signaling Technology, Beverly, MA). Results were normalized to β-actin. MCF7, a breast cancer cell line known to express CITED1, was used for a CITED1-positive control. COS cell lysate was used as a negative control. For developmental specimens (fetal heart, kidneys, and liver), immunoprecipitation Western blot analysis was performed as previously described [17].

To evaluate differences in gene transcription of *CITED1* between EMEF and pure fetal histology hepatoblastoma specimens, we isolated and purified total RNA from snap-frozen tissues using RNAzol (Tel-Test Inc, Friendswood, TX) and RNeasy Mini Kits (Qiagen, Germantown, MD). Isolated RNA was quantified using a SpectraMax M5 UV spectrophotometer (Molecular Devices, Sunnyvale, CA). Reverse transcription (RT) of 3 μg of RNA was performed using Superscript II reverse transcriptase (Invitrogen, Grand Island, NY) and oligodT primers (Applied Biosystems, Foster City, CA) to synthesize cDNA suitable for analysis by quantitative real-time–polymerase chain reaction (qRT-PCR; Bio-Rad iCycler; Bio-Rad, Hercules, CA) using iQ SYBR Green Super Mix (Bio-Rad). For *Dickkopf-related protein 1* (*DKK1*), *Kringle containing transmembrane protein 1* (*KREMEN1*), *CXXC finger protein 4* (*CXXC4*), and *PCNA*, qRT-PCR was performed using TaqMan probe–based gene expression analysis (Applied Biosystems). Changes in mRNA expression were determined by comparison of sample cycle threshold values against a standard curve generated using plasmid or positive control sample cDNA. Results were normalized to the housekeeping gene *GAPDH* and compared statistically. Primer sequences used for these studies are supplied in Table W1.

To determine the mutational status of the *CTNNB1* gene in the hepatoblastoma samples provided by the COG, we amplified cDNA with Taq polymerase using provided primer sequences flanking exons 1 to 5 of the *CTNNB1* gene (Table W1). Each reaction for the primers covering exons 2 to 4 comprised 1× PCR buffer (Sigma-Aldrich, St Louis, MO), 200 mM dNTP, 400 nM of each primer, and 0.05 units/ml Taq polymerase (Sigma-Aldrich); each reaction for the primer set of exons 1 to 5 comprised 1× PCR buffer (Promega, Madison, WI), 200 mM dNTP, 300 nM of each primer, 1% DMSO, 1 mM $MgCl_2$, and 2.5 units GoTaq Flexi DNA polymerase (Promega). Cycling conditions were given as follows: 1) initial denaturation at 94°C for 3 minutes; 2) 42 cycles at 94°C for 40 seconds, 54°C for 40 seconds, and 72°C for 50 seconds; and 3) final elongation at 72°C for 10 minutes. PCR products were gel purified using a QIAquick Gel Extraction Kit (Qiagen, Valencia, CA) and subsequently directly sequenced by GeneHunter Corporation (Nashville, TN). Generated sequences and chromatographs were compared to wild-type CTNNB1 using the Basic Local Alignment Search Tool (BLAST; NCBI, Bethesda, MD) to determine the mutational status of each specimen. These methods could not determine the mutational status of four tumors from the COG, leaving a total of 15 tumors analyzed for *CTNNB1* mutations. Base-pair references are made with respect to sequence NM_001904 for *CTNNB1*.

To assess the effect of CITED1 overexpression on Wnt signaling in hepatoblastoma, we isolated and quantified RNA from four consecutive passages of both Hep293TT-pcDNA3 cells and Hep293TT-CITED1 cells using techniques described above. Reverse transcription (RT) was

performed with 1 μg of RNA using the RT^2 First Strand cDNA Synthesis Kit (SA Biosciences, Frederick, MD). The RT^2 Profiler PCR array specific for the Wnt signaling pathway (PAHS-043A) was purchased from SA Biosciences and used according to the manufacturer's instructions. This array provides quantitative analysis of 84 Wnt pathway components and target genes with expression normalized to a panel of five housekeeping genes on a 96-well plate format.

CITED1 Misexpression Studies

CITED1 was misexpressed in the human hepatoblastoma cell line, Hep293TT, using the Fugene HD cell transfection reagent (Promega) [23]. An N-terminal FLAG-tagged CITED1 construct was inserted into pCDNA3 vector (Invitrogen) containing a neomycin-resistance cassette [24]. Subconfluent cells were transfected using 1 μg of plasmid DNA. Seventy-two hours after transfection, 0.3 μg/ml G418 sulfate (Sigma Chemical Co) was added to select for transfected cells. Resulting pooled colonies were isolated and passaged over a 6-week period to foster generation of stable cell lines. Two stable cell lines were generated: 1) empty-vector control cells, Hep293TT-pcDNA, and 2) a CITED1 overexpression cell line, Hep293TT-CITED1. Absence or expression of CITED1 was verified by immunofluorescence and Western blot.

In Vitro *Studies: Proliferation and Soft Agar Assays*

In vitro effects of CITED1 overexpression on cellular proliferation were assayed by 3-(4,5-dimethylthiazol-2-yl)-2,5-diphenyltetrazolium bromide (MTT) incorporation using the CellTiter 96 Non-Radioactive Cell Proliferation Assay (Promega). The two aforementioned cell lines were plated in starvation medium (ACL-4 media with 0.2% FBS) [25] for 24 hours before experimentation. The cells were then harvested and 5×10^4 cells were plated in 200 μl of ACL-4 media [25] with 0.2% FBS in four wells for each cell line at each time point tested. MTT was added and quenched as per the manufacturer's instructions. Incorporation was assayed at 0, 24, 48, and 72 hours using spectrophotometry. Absorbances were compared statistically. Results represent four experimental repeats.

In vitro effects of CITED1 overexpression on anchorage-independent growth were determined using soft agar assays. Twenty thousand cells from each described cell line were plated in six separate wells of a six-well plate in SeaPlaque GTG Agarose (Lonza, Rockland, ME) in ACL-4 media (0.8% bottom agar and 0.4% top agar). Agars were covered in 200 μl of ACL-4 media and allowed to incubate for 3 weeks. Colony counts and sizes were assayed using MTT staining and quantified using a GelCount system (Oxford Optronix, Oxford, United Kingdom). Results represent three experimental repeats.

Statistical Analysis

The incidence of strong [immunohistochemistry (IHC) score of 2 *vs* 0 or 1] CITED1 expression was compared between EMEF and pure fetal histology specimens overall, in the cytosol, and in the nucleus using Fisher exact test. The monotonic association between *CITED1* and *PCNA* mRNA expression was estimated using the Spearman correlation with 95% confidence intervals estimated by bootstrapping (10,000 replicates). The Wilcoxon rank sum test was used to compare the differences of normalized gene expression between the EMEF and pure fetal histology hepatoblastomas for both qRT-PCR and Western blot and to compare colony size and counts for the soft agar assay for anchorage independent growth. Two-way analysis of variance was used to compare proliferation profiles of Hep293TT-CITED1 to Hep293TT-pcDNA3 cells over time using data generated by the MTT proliferation assay, and this experiment was independently replicated four times. A statistically significant ($P < .0001$) interaction between treatment and time was detected among all four experiments. Consequently, group comparisons were made at each time point in all four experiments. Although we controlled the overall type I error at 0.05 for all 16 time points (4 time points in each of four experiments) using the method of Holm [26], only one experiment is presented. Statistical analysis from the RT^2 Profiler PCR array specific for the Wnt signaling pathway (PAHS-043A) was performed using the manufacturer's statistical software (SA Biosciences). All other analyses were performed using R 2.13.1 (R Development Core Team, Vienna, Austria). Statistical tests resulting in a P value less than .05 were considered statistically significant.

Results

Developmental Domains of CITED1 Expression

To determine the *CITED1* expression domain across development, we inspected whole-mount embryos at e11.5 from *CITED1*^{LacZ} reporter mice. This analysis demonstrated β-galactosidase expression in the heart, limbs, tail bud, and head mesenchyme (Figure 1) as previously described [27]. There is strong β-galactosidase staining in the fetal liver at this stage of development (Figure 1). Expression in the early metanephric kidney is obscured by the hind limb. To determine more precisely when and where CITED1 is expressed during liver development, we used immunohistochemistry to localize CITED1 protein using an affinity-purified rabbit polyclonal antibody that we have previously shown is highly specific for CITED1 [9]. CITED1 was not detected at e9.5 in the murine liver diverticulum, an outpouching of the ventral foregut endoderm (Figure 2*A*). At e10.5, CITED1 expression was detected in the liver bud (Figure 2*B*). Strong CITED1 expression persisted during maturation of the liver bud from

Figure 1. (A) *CITED1*^{LacZ} reporter mouse embryo at e11.5 gestation reveals expression of CITED1 in the second branchial arch (white arrow), fetal heart (white arrowhead), and fetal liver (black arrowheads). The hind limb obscures the metanephric kidney in this projection. fl = forelimb; hl = hind limb.

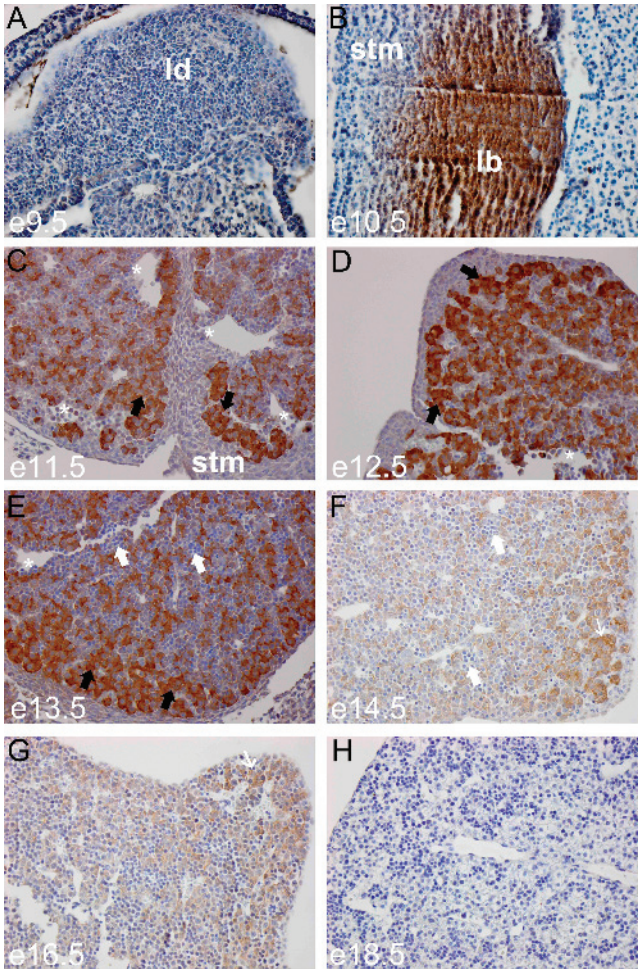

Figure 2. (A) CITED1 is not detected by immunohistochemistry at e9.5 of murine hepatic development, during the period of hepatic specification as the liver diverticulum (ld) forms (hepatoblasts delaminate) from the ventral foregut endoderm. (B) By e10.5, CITED1 is strongly detected in the proliferating hepatic bud and not detected in the adjacent septum transversum mesenchyme (stm). (C) At e11.5, CITED1 is strongly detected in hepatoblasts, which form hepatic cords (black arrows) following their invasion of the septum transversum mesenchyme. Sinusoids are also seen (white asterisks). (D and E) CITED1 remains strongly detected at e12.5 and e13.5. Hepatoblasts, black arrows; hematopoietic cells, white arrows. (F and G) CITED1 expression begins to taper at e14.5 to e16.5, when CITED1-negative invading hematopoietic cells can be seen (white arrows) and the nuclear-to-cytoplasmic ratio of the hepatoblasts begins to decrease (thin white arrow). (H) CITED1 expression is not detected by e18.5, when hepatic cells have a low nuclear-to-cytoplasmic ratio and have the appearance of fetal hepatocytes [original magnification, ×400 (A–H)].

e11.5 to e13.5 (Figure 2, *C–E*). CITED1 expression then tapered between e14.5 and 16.5, at which point invading hematopoietic cells were detected and the nuclear to cytosolic ratio of the CITED1-positive hepatocytes began to decrease (Figure 2, *F* and *G*). CITED1 expression was not detected at e18.5, when the epithelial cells of the fetal liver had a greatly decreased nuclear-to-cytoplasmic ratio typical of maturing fetal hepatocytes (Figure 2*H*).

Consistent with immunohistochemical data, CITED1 was detected in the fetal liver strongly by immunoprecipitation Western blot at e13.5 but tapered by e16.5 and was undetectable in e19.5 livers (Figure 3*A*). Interestingly, these data also show that CITED1 antibodies detect distinct mobility bands in embryonic liver *versus* heart and kidney. High molecular weight bands detected in embryonic hearts at e13.5 collapse to a single 27-kDa band when lysates are treated with alkaline phosphatase (data not shown). This is consistent with previous studies indicating that CITED1 undergoes regulated phosphorylation events [24]. The functional role of these phosphorylation events is unknown. However, CITED1 immunolocalization studies in e12.5 mouse embryos show cytosolic expression of CITED1 in the metanephric mesenchyme surrounding the ureteric bud tip epithelium (Figure 3*B*) and in hepatoblasts of the liver bud (Figure 3*D*) but nuclear expression of CITED1 in the trabeculae of the developing heart (Figure 3*C*). This suggests that cardiac-specific CITED1 phosphorylation could play a role in regulating CITED1 subcellular localization.

CITED1 Expression in an Experimental Murine Model of Hepatoblastoma

Because of its expression in hepatic development, we next asked whether CITED1 could also be detected in hepatoblastoma, a childhood malignancy that is characterized by cells with an embryonal and abnormal progenitor-like phenotype. We started by testing for the presence of CITED1 in an experimental murine model of hepatoblastoma. Chemically induced mouse hepatoblastomas were investigated for CITED1 expression by immunohistochemistry [21]. CITED1 was detected in 40 of 43 tumors (93% of experimental hepatoblastomas analyzed; Figure 4, *A* and *B*). Unexpectedly, CITED1 was also detected in adjacent areas of hepatic parenchymal injury and often coincided with areas of steatosis (Figure 4, *C* and *D*). Because we noted intense CITED1 staining in these areas of hepatic parenchymal injury, we wanted also to determine whether CITED1 reactivation occurred in other models of hepatic injury associated with liver regeneration. We tested tissue sections from murine partial hepatectomy specimens and murine livers treated with DDC, an inhibitor of heme biosynthesis that leads to accumulation of porphyrin and induces oval cell proliferation,

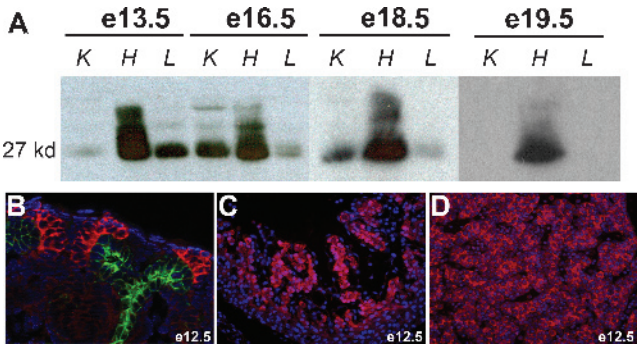

Figure 3. (A) Immunoprecipitation (IP)-Western blot for CITED1 in e13.5, e16.5, e18.5, and e19.5 murine fetal kidney (K), heart (H), and liver (L). Liver expression of CITED1 is strong at e13.5, but tapers between e16.5 and 18.5, and is no longer detected by e19.5. Time course of CITED1 expression in the kidney and heart is shown for comparison. (B) Cytosolic detection of CITED1 is seen in the e12.5 murine fetal kidney cap mesenchyme (pink) surrounding the ureteric bud tip epithelium, which shows characteristic expression of cytokeratin 8 (green). (C) Nuclear detection of CITED1 in the trabeculae of the developing heart at e12.5. (D) Cytosolic expression of CITED1 in hepatoblasts at e12.5 [original magnification ×400 (B and D)].

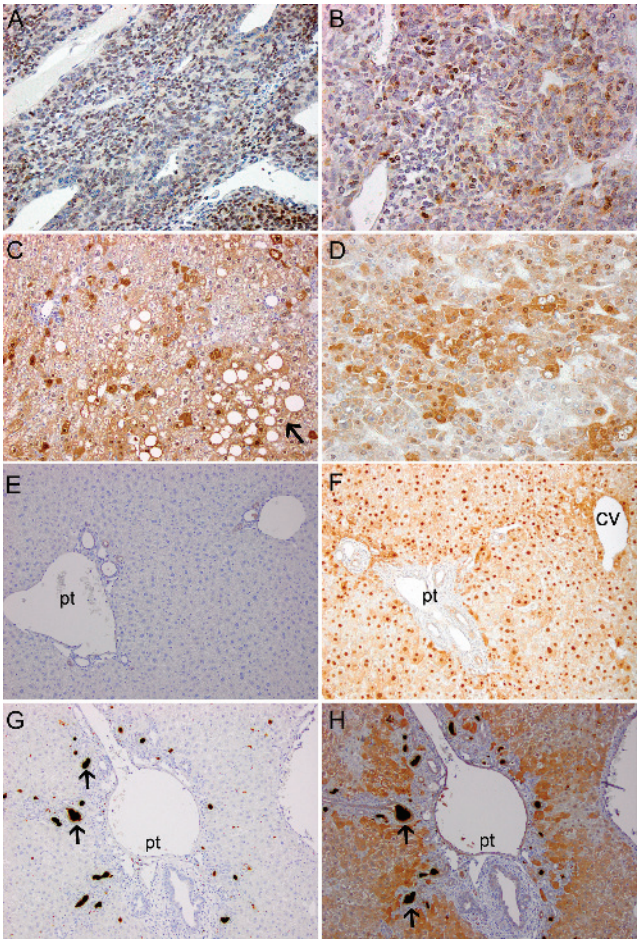

Figure 4. (A and B) Detection of CITED1 in the *N*-nitrosodiethylamine, 2,3,7,8-tetrachlorodibenzo-*p*-dioxin murine model of hepatoblastoma. (C and D) CITED1-positive areas of injured liver in the *N*-nitrosodiethylamine, 2,3,7,8-tetrachlorodibenzo-*p*-dioxin murine model often coincided with areas of hepatic steatosis (black arrow); original magnification, ×200. (E) Normal, uninjured murine liver is negative for CITED1. (F) Nuclear enrichment of CITED1 is observed by immunohistochemistry at 7 days post-murine partial hepatectomy surrounding portal triads (pt) and central veins (cv). (G) IgG control of DDC induced murine liver injury. Note porphyrin accumulation (black arrows) characteristic of this injury model. (H) CITED1 is detected in DDC injured mouse liver 21 days post-exposure, and expression is enriched surrounding portal triads but not clearly central veins; original magnification, ×200 (A–H).

the proposed progenitor cell of the adult liver [22]. CITED1 reactivation was detected in all cases, particularly surrounding portal triads in both the partial hepatectomy and DDC models and surrounding both portal triads and central veins in the partial hepatectomy model (Figure 4, *F* and *H*).

Immunohistochemical Detection of CITED1 in Human Hepatoblastoma

We next tested the presence of CITED1 in human hepatoblastoma specimens. CITED1 was detected by immunohistochemistry in 36 of 41 (87.8%) specimens analyzed. Of note, the six specimens in which CITED1 was not detected were all of pure fetal histology (Figure 5*A*). CITED1 was observed strongly in embryonal areas of EMEF histology hepatoblastomas (Figure 5, *B*–*F*). Overall, CITED1 was strongly expressed in 23 of 28 (82.1%) EMEF histology tumors compared to 1 of 13 pure fetal histology tumors (Fisher exact test; $P < .0001$). Nuclear expression was strong in 11 (39.3%) of 28 EMEF histology samples, whereas none of the pure fetal samples expressed nuclear CITED1 strongly (Fisher exact test; $P < .009$). Strong cytosolic expression of CITED1 was expressed in 23 of 28 EMEF histology tumors compared to 1 of 13 pure fetal histology tumors (Fisher exact test; $P < .0001$). Often, areas of abrupt transition in CITED1 expression correlated with the juxtaposition of embryonal and fetal histology in EMEF

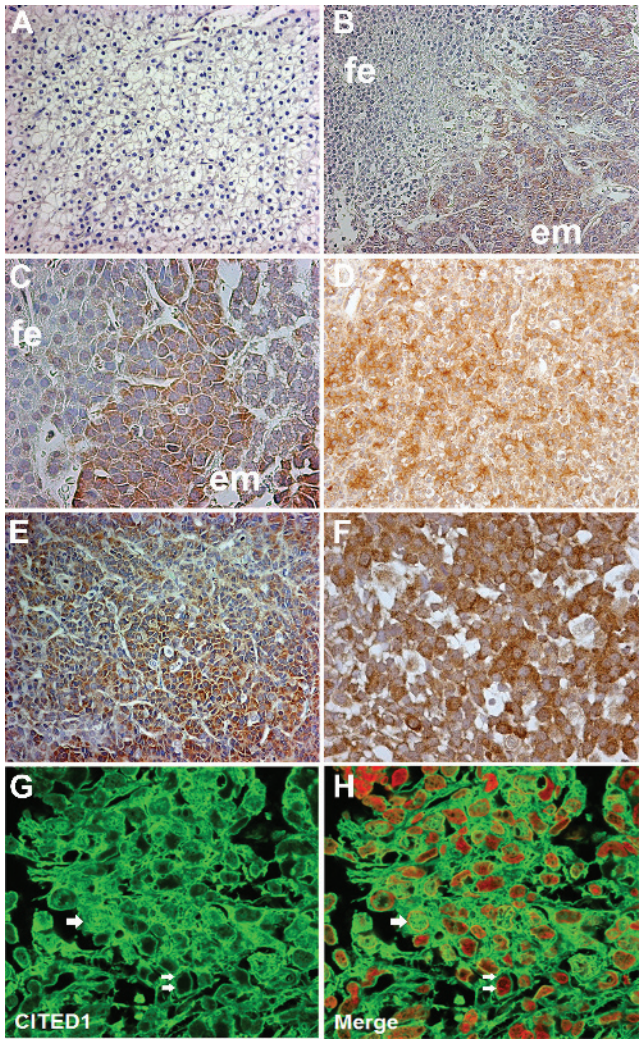

Figure 5. (A) Pure fetal histology hepatoblastomas often did not show immunohistochemical detection of CITED1; original magnification, ×200. (B) In EMEF tumors, CITED1 expression was more greatly detected in embryonal (em) elements, when compared to fetal (fe) elements; original magnification, ×200. (C) High power representation of transition between embryonal and fetal elements; original magnification, ×400. (D) An EMEF histology hepatoblastoma exhibiting CITED1 expression in embryonal and fetal elements; original magnification, ×200. (E and F) CITED1 is richly detected in the embryonal elements of EMEF histology tumors [original magnification, ×200 (E); ×400 (F)]. (G) Immunofluorescence shows dysregulated nuclear (single white arrows) and cytosolic (double white arrows) subcellular localization of CITED1 in hepatoblastoma. (H) Merged image of CITED1 (green) and TOPRO3 nuclear stain (red) [original magnification, ×400 (G and H)].

histology tumors (Figure 5, *B* and *C*). By immunofluorescence, we observed both cytosolic and nuclear expression of CITED1 in hepatoblastoma (Figure 5, *G* and *H*).

Quantification of CITED1 Expression in Pure Fetal and EMEF Histology Hepatoblastomas

To test the hypothesis that *CITED1* expression is greater in more undifferentiated tumors, we performed qRT-PCR and Western blot analysis on hepatoblastomas provided by the COG. While expression of *CITED1* mRNA was similar between EMEF and pure fetal histology tumors (Figure 6*A*), we did detect a marginal increase in CITED1 expression by Western blot for EMEF histology specimens (Wilcoxon rank sum test; $P = .085$; Figure 6, *B* and *C*).

Functional Significance of CITED1 Overexpression in Human Hepatoblastoma Cells

To investigate the possible function of CITED1 in hepatoblastoma pathogenesis, we established stable Hep293TT human hepatoblastoma cell lines expressing either epitope-tagged CITED1 or empty vector control. The presence and absence of both CITED1 and FLAG expression in these experimental cell lines were confirmed by Western blot (see Figure 8*A*) and immunofluorescence confirmed expression in all of the selected cells (data not shown).

CITED1 overexpression resulted in a statistically significant increase in cell numbers as determined by MTT proliferation assay by 48 and 72 hours after assay initiation in all four experiments; in three of four experiments, this difference was also statistically significant at 24 hours (Figure 7*A*; Holm-Bonferroni method; $P < .05$ all time points). Decreased MTT detection in the control cell line initially indicates potential death of control cells in serum-starved conditions. CITED1 overexpression did not, however, significantly affect colony size or colony count when compared to Hep293TT-pcDNA3 empty vector control cells by soft agar assay for anchorage-independent growth (Wilcoxon rank sum test; $P = .083$ colony size; $P = .563$ colony count). To validate this association between CITED1 overexpression and increased hepatoblastoma cellular proliferation, we tested for a correlation between increasing *CITED1* and *PCNA* mRNA expression in human hepatoblastoma patient specimens. In the 19 hepatoblastomas provided by the COG, we detected a statistically significant positive correlation between increasing *CITED1* and *PCNA* mRNA expression (Spearman correlation coefficient = 0.554; 95% confidence interval (CI) = 0.061–0.858; $P = .015$; Figure 7*B*). CITED1 and PCNA expression localized to similar cellular expression domains by immunohistochemical staining of serial hepatoblastoma tissue sections (Figure 7, *C–F*).

Given the potential role of CITED1 as an inhibitor of the Wnt pathway from previous studies and the importance of dysregulated Wnt signaling in hepatoblastoma pathogenesis [28], we tested whether CITED1 overexpression altered Wnt signaling in human hepatoblastoma cells. Using the RT^2 Profiler PCR array specific for the Wnt signaling pathway (SA Biosciences), four biologic replicates (passages) of Hep293TT-CITED1 cells showed significant up-regulation of the Wnt inhibitors *KREMEN1* and *CXXC4* ($P = .034$ and .043, respectively) and also the Wnt effector *DVL2* ($P = .042$) when compared to Hep293TT-pcDNA3 empty vector control cells (Figure 8*B*). Complete array data are provided (Tables W2a–W2g). To validate these findings in the context of CITED1 overexpression in human hepatoblastomas *in vivo*, we tested for a correlation between *CITED1* mRNA expression and that of *KREMEN1* and *CXXC4* in human hepatoblastoma patient specimens. In the 19 hepatoblastomas provided by the COG, we detected a statistically significant positive correlation between increasing *CITED1* and *CXXC4* mRNA expression (Spearman

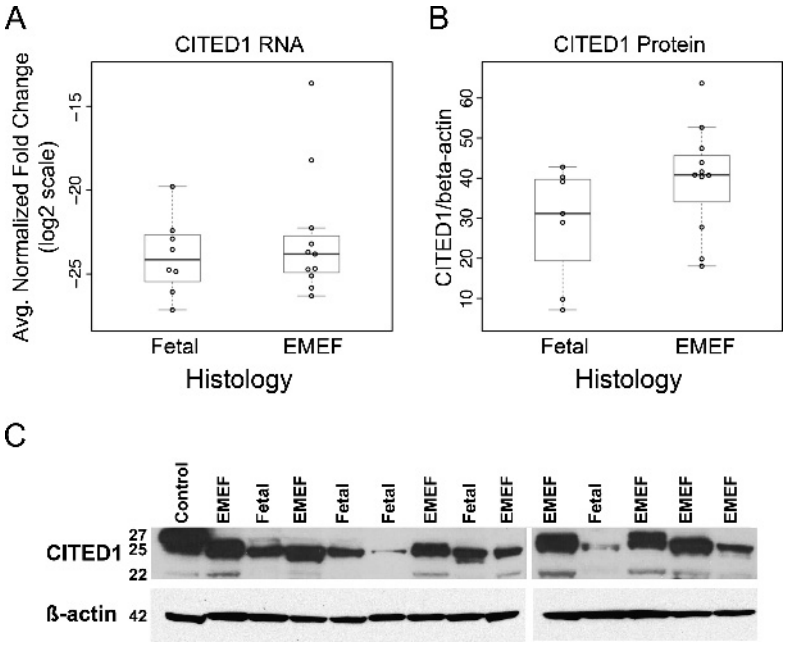

Figure 6. (A) While the highest CITED1-expressing tumors were EMEF histology, there was no difference in mean *CITED1* expression detected by qRT-PCR normalized to β-actin (P = NS). (B) CITED1 expression was marginally higher in EMEF histology specimens by Western blot densitometry normalized to β-actin ($P = .085$). (C) Example of Western blot demonstrating increased CITED1 expression in hepatoblastoma specimens of EMEF histology. Positive control is MCF7 cell lysate, a breast cancer cell line that is known to express high levels of CITED1.

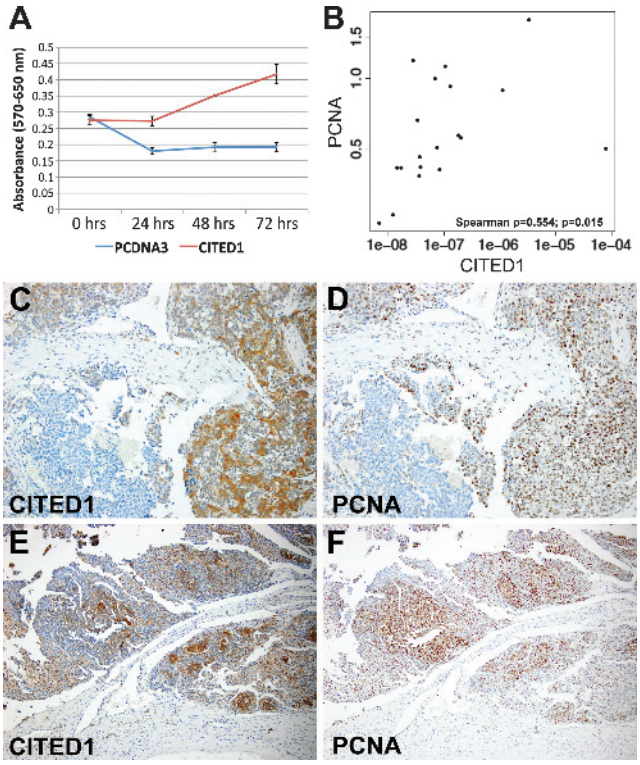

Figure 7. (A) An MTT cell proliferation assay in ACL-4 media with 0.2% FBS demonstrates a significant increase in cellular proliferation at 24, 48, and 72 hours with CITED1 overexpression (method of Holm-Bonferroni; $P < .05$). (B) qRT-PCR of human hepatoblastoma specimens reveals a positive correlation between expression of *CITED1* and the proliferative marker *PCNA* (Spearman correlation coefficient = 0.554; $P = .015$). (C and D) Serial hepatoblastoma tissue sections immunostained for (C) CITED1 and (D) PCNA demonstrate similar patterns of expression within a given tumor, supporting the correlation between CITED1 expression and cellular proliferation (original magnification, ×200). (E and F) Additional serial sections stained for (E) CITED1 and (F) PCNA (original magnification, ×100).

correlation coefficient = 0.521; 95% CI = 0.061–0.787 $P = .024$; Figure 7*C*). Likewise, we detected a significant positive correlation between increasing *CITED1* and *KREMEN1* mRNA expression (Spearman correlation coefficient = 0.553; 95% CI = 0.143–0.807 $P = .016$; Figure 7*D*). Because KREMEN1 is the DKK1 receptor, we also tested whether an association was present between *CITED1* and *DKK1*, which specifically has been shown to become dysregulated in hepatoblastoma [29]. Although no statistically significant correlation was detected between *CITED1* and *DKK1* expression in these clinical specimens (Spearman correlation coefficient = 0.23; $P = .342$; Figure 7*E*), we did note a statistically significant increase in *DKK1* expression in mixed-epithelial histology relative to pure fetal histology specimens (Wilcoxon rank sum test; $P = .003$; Figure 7*F*).

CITED1 Expression and CTNNB1 Mutational Status

Given the detected correlations between *CITED1* expression and components of the Wnt pathway, we determined the mutational status of *CTNNB1* in hepatoblastoma specimens provided by the COG by sequencing exons 1 to 5 from cDNA samples reverse transcribed from isolated RNA (Table W3). Ten of 15 (66.7%) hepatoblastoma specimens were found to have a *CTNNB1* mutation. Seven of 10 (70%) *CTNNB1* mutant hepatoblastoma specimens were EMEF histology, whereas 3 of 10 (30%) were of pure fetal histology ($P = .957$). Mean CITED1 expression by Western blot densitometry normalized to β-actin was not statistically different between *CTNNB1* mutant and wild-type groups ($P = .817$). However, by Western blot densitometry normalized to β-actin, there was a statistically significant correlation between CITED1 and β-catenin expression (Spearman correlation coefficient = 0.52; $P = .033$). CITED1 and β-catenin also had similar regions of expression within a given tumor by immunohistochemical staining of serial tumor sections (Figure W1).

Discussion

Our data show that CITED1 is expressed in developing hepatoblasts during maturation of the liver bud and tapers off as these cells differentiate into hepatocytes. Analogous to this embryonic context, CITED1 expression appeared greatest in the undifferentiated embryonal tumor elements of mixed-epithelial hepatoblastoma. Prognostically more favorable pure fetal histology tumors, and even the more differentiated fetal areas of EMEF histology tumors, showed lower expression of CITED1. In addition, as previously described in renal progenitor cells and WT [17], the subcellular localization of CITED1 is dysregulated in hepatoblastoma when compared to its predominantly cytosolic localization in hepatic development. Functionally, CITED1 overexpression in human hepatoblastoma cells increases cellular proliferation but does not affect tumorigenesis *in vitro*, as measured by soft agar assay of anchorage-independent growth. Proliferation of cells in which CITED1 was overexpressed was often accompanied by apparent cell death in the control group cells, potentially indicating a survival advantage conferred by CITED1 overexpression in low-serum conditions consistent with cell stress. The association between CITED1 activity and cellular proliferation was also apparent in hepatoblastoma clinical specimens. CITED1 was further detected in a nitrosamine and aromatic hydrocarbon–induced murine model of hepatoblastoma;

Figure 8. (A) Western blot demonstrates overexpression of CITED1 and detection of epitope-tagged CITED1 (FLAG) in Hep293TT human hepatoblastoma cells transfected with FLAG-tagged wild-type CITED1 (Hep293TT-CITED1) compared to empty vector control plasmid (Hep293TT-pcDNA3). Positive control is MCF7 breast cancer cell line and negative control is COS cell line. (B) qRT-PCR using a Wnt-PCR array revealed a statistically significant increase in fold change of the Wnt inhibitors *CXXC4* ($\log_2$ fold change = 2.88) and *KREMEN1* ($\log_2$ fold change = 1.60) and also the Wnt effector *DVL2* ($\log_2$ fold change = 1.21) after CITED1 overexpression. (C and D) qRT-PCR of human hepatoblastoma specimens reveals a correlation between expression of (C) *CITED1* and the Wnt inhibitor *CXXC4* (Spearman correlation coefficient = 0.521; $P = .024$) and (D) *CITED1* and the Wnt inhibitor *KREMEN1* (Spearman correlation coefficient 0.553; $P = .016$). (E) No correlation was detected in clinical hepatoblastoma specimens between expression of *CITED1* and the *KREMEN1* ligand *DKK1* (Spearman correlation coefficient = 0.23; $P = .342$). (F) However, *DKK1* was found to be expressed greater in EMEF histology than pure fetal histology hepatoblastoma specimens ($P = .003$).

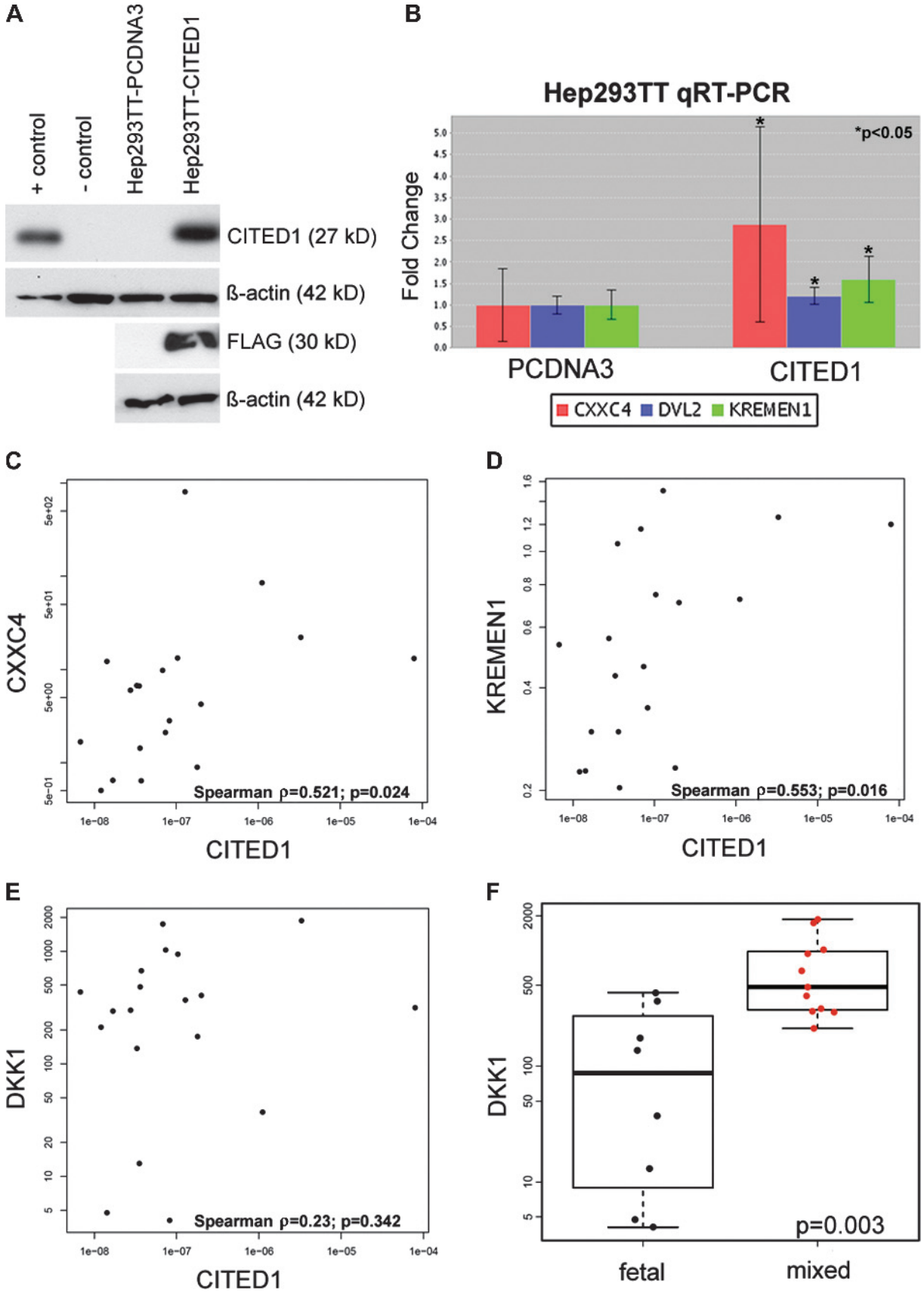
A
+ control
- control
Hep293TT-PCDNA3
Hep293TT-CITED1
CITED1 (27 kD)
ß-actin (42 kD)
FLAG (30 kD)
ß-actin (42 kD)
B
Hep293TT qRT-PCR
Fold Change
*p<0.05
PCDNA3
CITED1
CXXC4 DVL2 KREMEN1
C
CXXC4
CITED1
Spearman ρ=0.521; p=0.024
D
KREMEN1
CITED1
Spearman ρ=0.553; p=0.016
E
DKK1
CITED1
Spearman ρ=0.23; p=0.342
F
DKK1
p=0.003
fetal
mixed

however, we also saw reactivation of CITED1 expression in surrounding areas of hepatic parenchymal injury, providing additional evidence for a possible reactivation of embryonal transcriptional programs in liver injury and regeneration. Reactivation of CITED1 expression associated with hepatic injury and regeneration was confirmed after murine partial hepatectomy and DDC treatment, which both induce oval cell proliferation, a key marker of hepatic regeneration. Taken together, we speculate that CITED1 expression in hepatoblastomas either persists postnatally or becomes reactivated in the neoplastic transformation from progenitor to cancer cell, as inferred from the chemically induced murine model.

CITED1 expression has not been previously reported in human or murine liver development, although the related family member, CITED2, is critical for hepatic development through its interactions with hepatocyte nuclear factor-alpha 4 (HNF-α 4), a required transcription factor for epithelial differentiation in the developing liver [30]. Although expression of CITED1, from our study, appears to adhere to a similar developmental time frame to that reported for CITED2, *CITED1* null mice do not exhibit any overt hepatic morphologic or histologic abnormalities (data not shown), implying functional redundancy of signaling similar to what has been observed in nephrogenesis [9]. While *CITED1* null mice do exhibit decreased hepatic mass relative to controls, this is caused by asymmetric intrauterine growth retardation secondary to placental insufficiency [31].

The Wnt signaling pathway has been implicated in maintaining the critical, coordinated balance between differentiation and proliferation in multiple developmental contexts, particularly in the developing liver [6]. Wnt/β-catenin plays a biphasic role in hepatic development, with suppression of signaling until after the period of hepatic specification, followed by increased signaling driving the proliferation of hepatoblasts [6]. Specifically, coordinated control of Wnt signaling has been linked to the transcriptional co-activators, CBP and P300, which are the principal proteins with which CITED1 interacts [32,33]. CITED1 may therefore participate as a co-regulator in the modulation and balance of CBP/β-catenin–mediated transcription critical for stem/progenitor cell maintenance and P300/β-catenin–mediated transcription important in the initiation of cellular differentiation.

Disruption of balanced Wnt signaling is critical in hepatoblastoma pathogenesis, with between 50% and 90% of hepatoblastomas harboring β-catenin mutations [7,8]. Despite activated and pro-proliferative Wnt signaling being a dominant feature in hepatoblastoma, elevation of multiple Wnt antagonists including TrCP, Nkd-1, AXIN2, and DKK1 have been previously reported, possibly signifying a nonfunctional negative feedback loop [29,34]. Because CITED1 is a potential repressor of the Wnt pathway [11], we evaluated the effects *in vitro* of overexpressing CITED1 on Wnt pathway genes. In these studies, we found that CITED1 overexpression was associated with up-regulation of two key components of Wnt signaling inhibition: *KREMEN1* and *CXXC4*. We validated these findings in clinical hepatoblastoma specimens, which revealed that *CITED1* mRNA expression correlated positively with the Wnt components, *KREMEN1* and *CXXC4*, independent of histologic subtype. *DKK1* expression (another inhibitor of Wnt signaling) did not correlate with *CITED1* mRNA expression but increased in association with mixed (more embryonal) histology. These findings implicate CITED1 as a modulator of Wnt signaling in hepatoblastoma and possibly also liver development. The seemingly paradoxical role of CITED1-promoted increased cellular proliferation and Wnt inhibition in the malignant context implies, analogously, a persistent developmental role, which may be specific to stem-like cells, whether embryonic progenitors or a cancer stem cell. Speculatively, CITED1 may modulate Wnt signaling to simultaneously promote or inhibit differentiation and maintenance/proliferation of the progenitor cell pool in a developing organ.

From these studies, the detection of CITED1 in hepatoblastoma appears to be linked to undifferentiated, embryonal tumor elements. We detected increased CITED1 by immunohistochemistry in EMEF histology hepatoblastomas containing both embryonal and fetal elements when compared to more differentiated, pure fetal histology hepatoblastomas. This observation was not statistically supported by qRT-PCR, whereas a marginally significant increase was detected by Western blot. CITED1 expression appeared to inversely correlate with tumor differentiation, a finding that may have prognostic importance given that pure fetal histology hepatoblastomas exhibit favorable behavior and are able to be treated by surgical resection alone without chemotherapy. Furthermore, we detected an association between the Wnt inhibitor *DKK1* mRNA expression and mixed-epithelial histology tumors. Taken together, these results suggest that CITED1 may confer a survival advantage to the more primitive cellular components of hepatoblastoma by enhancing proliferation independent of oncogenic behavior and may further promote maintenance of stem-like properties in this embryonal malignancy by inhibiting Wnt-dependent mechanisms of cellular differentiation.

The role of CITED1 as a marker of the self-renewing stem cell population in kidney development and the promotion of cellular proliferation by CITED1 overexpression in human hepatoblastoma cells in the current study perhaps suggest a role for CITED1 in cancer cell self-renewal. Its role as a marker of hepatoblasts before epithelial transition and its link to undifferentiated tumor elements may implicate CITED1 in a network of gatekeepers that inhibit developmental progenitor or embryonal tumor cell differentiation. Therefore, CITED1 and its associated pathways may provide fertile ground for potential pathway-targeted therapies that abrogate cancer cell self-renewal or promote terminal differentiation of embryonal tumors.

Acknowledgments

We acknowledge the excellent services of the COG Biopathology Center, which were instrumental in specimen acquisition and data analysis, and also the NCI-funded Human Tissue Acquisition and Pathology Shared Resource at Vanderbilt (grant P30 CA68485). We also acknowledge Julia Kutaka and Jennifer Westrup Slone for their contributions to the experiments described herein. We were graciously provided the Hep293TT human hepatoblastoma cell line from the laboratory of Tina Chen and Gail Tomlinson and experimental murine hepatoblastoma specimens from the laboratory of Lucy Anderson.

References

[1] Litten JB and Tomlinson GE (2008). Liver tumors in children. *Oncologist* **13**, 812–820.

[2] Malogolowkin MH, Katzenstein HM, Meyers RL, Krailo MD, Rowland JM, Haas J, and Finegold MJ (2011). Complete surgical resection is curative for children with hepatoblastoma with pure fetal histology: a report from the Children's Oncology Group. *J Clin Oncol* **29**, 3301–3306.

[3] Scotting PJ, Walker DA, and Perilongo G (2005). Childhood solid tumours: a developmental disorder. *Nat Rev Cancer* **5**, 481–488.

[4] Ruck P and Xiao JC (2002). Stem-like cells in hepatoblastoma. *Med Pediatr Oncol* **39**, 504–507.

[5] Ruck P, Xiao JC, and Kaiserling E (1996). Small epithelial cells and the histogenesis of hepatoblastoma. Electron microscopic, immunoelectron microscopic, and immunohistochemical findings. *Am J Pathol* **148**, 321–329.

[6] Si-Tayeb K, Lemaigre FP, and Duncan SA (2010). Organogenesis and development of the liver. *Dev Cell* **18**, 175–189.
[7] Jeng YM, Wu MZ, Mao TL, Chang MH, and Hsu HC (2000). Somatic mutations of β-catenin play a crucial role in the tumorigenesis of sporadic hepatoblastoma. *Cancer Lett* **152**, 45–51.
[8] Wei Y, Fabre M, Branchereau S, Gauthier F, Perilongo G, and Buendia MA (2000). Activation of β-catenin in epithelial and mesenchymal hepatoblastomas. *Oncogene* **19**, 498–504.
[9] Boyle S, Shioda T, Perantoni AO, and de Caestecker M (2007). Cited1 and Cited2 are differentially expressed in the developing kidney but are not required for nephrogenesis. *Dev Dyn* **236**, 2321–2330.
[10] Hendry C, Rumballe B, Moritz K, and Little MH (2011). Defining and redefining the nephron progenitor population. *Pediatr Nephrol* **26**, 1395–1406.
[11] Plisov S, Tsang M, Shi G, Boyle S, Yoshino K, Dunwoodie SL, Dawid IB, Shioda T, Perantoni AO, and de Caestecker MP (2005). Cited1 is a bifunctional transcriptional cofactor that regulates early nephronic patterning. *J Am Soc Nephrol* **16**, 1632–1644.
[12] Dressler GR (2009). Advances in early kidney specification, development and patterning. *Development* **136**, 3863–3874.
[13] Li CM, Guo M, Borczuk A, Powell CA, Wei M, Thaker HM, Friedman R, Klein U, and Tycko B (2002). Gene expression in Wilms' tumor mimics the earliest committed stage in the metanephric mesenchymal-epithelial transition. *Am J Pathol* **160**, 2181–2190.
[14] Davidoff AM (2009). Wilms' tumor. *Curr Opin Pediatr* **21**, 357–364.
[15] Li CM, Kim CE, Margolin AA, Guo M, Zhu J, Mason JM, Hensle TW, Murty VV, Grundy PE, Fearon ER, et al. (2004). CTNNB1 mutations and overexpression of Wnt/β-catenin target genes in WT1-mutant Wilms' tumors. *Am J Pathol* **165**, 1943–1953.
[16] Huff V (2011). Wilms' tumours: about tumour suppressor genes, an oncogene and a chameleon gene. *Nat Rev Cancer* **11**, 111–121.
[17] Lovvorn HN, Westrup J, Opperman S, Boyle S, Shi G, Anderson J, Perlman EJ, Perantoni AO, Wills M, and de Caestecker M (2007). CITED1 expression in Wilms' tumor and embryonic kidney. *Neoplasia* **9**, 589–600.
[18] Murphy AJ, Pierce J, de Caestecker C, Taylor C, Anderson JR, Perantoni AO, de Caestecker MP, and Lovvorn H III (2011). SIX2 and CITED1, markers of nephronic progenitor self-renewal, remain active in primitive elements of Wilms' tumor. *J Pediatr Surg* **47**, 1239–1249.
[19] Lovvorn HN III, Boyle S, Shi G, Shyr Y, Wills ML, Perantoni AO, and de Caestecker M (2007). Wilms' tumorigenesis is altered by misexpression of the transcriptional co-activator, CITED1. *J Pediatr Surg* **42**, 474–481.
[20] Sado T, Fenner MH, Tan SS, Tam P, Shioda T, and Li E (2000). X inactivation in the mouse embryo deficient for *Dnmt1*: distinct effect of hypomethylation on imprinted and random X inactivation. *Dev Biol* **225**, 294–303.
[21] Beebe LE, Fornwald LW, Diwan BA, Anver MR, and Anderson LM (1995). Promotion of *N*-nitrosodiethylamine-initiated hepatocellular tumors and hepatoblastomas by 2,3,7,8-tetrachlorodibenzo-*p*-dioxin or Aroclor 1254 in C57BL/6, DBA/2, and B6D2F1 mice. *Cancer Res* **55**, 4875–4880.
[22] Wang X, Foster M, Al-Dhalimy M, Lagasse E, Finegold M, and Grompe M (2003). The origin and liver repopulating capacity of murine oval cells. *Proc Natl Acad Sci USA* **100**(suppl 1), 11881–11888.
[23] Chen TT, Rakheja D, Hung JY, Hornsby PJ, Tabaczewski P, Malogolowkin M, Feusner J, Miskevich F, Schultz R, and Tomlinson GE (2009). Establishment and characterization of a cancer cell line derived from an aggressive childhood liver tumor. *Pediatr Blood Cancer* **53**, 1040–1047.
[24] Shi G, Boyle SC, Sparrow DB, Dunwoodie SL, Shioda T, and de Caestecker MP (2006). The transcriptional activity of CITED1 is regulated by phosphorylation in a cell cycle-dependent manner. *J Biol Chem* **281**, 27426–27435.
[25] Masuda N, Fukuoka M, Takada M, Kudoh S, and Kusunoki Y (1991). Establishment and characterization of 20 human non-small cell lung cancer cell lines in a serum-free defined medium (ACL-4). *Chest* **100**, 429–438.
[26] Holm S (1979). A simple sequentially rejective Bonferroni test procedure. *Scand J Stat* **6**, 65–70.
[27] Dunwoodie SL, Rodriguez TA, and Beddington RS (1998). *Msg1* and *Mrg1*, founding members of a gene family, show distinct patterns of gene expression during mouse embryogenesis. *Mech Dev* **72**, 27–40.
[28] Armengol C, Cairo S, Fabre M, and Buendia MA (2011). Wnt signaling and hepatocarcinogenesis: the hepatoblastoma model. *Int J Biochem Cell Biol* **43**, 265–270.
[29] Wirths O, Waha A, Weggen S, Schirmacher P, Kuhne T, Goodyer CG, Albrecht S, Von Schweinitz D, and Pietsch T (2003). Overexpression of human Dickkopf-1, an antagonist of wingless/WNT signaling, in human hepatoblastomas and Wilms' tumors. *Lab Invest* **83**, 429–434.
[30] Qu X, Lam E, Doughman YQ, Chen Y, Chou YT, Lam M, Turakhia M, Dunwoodie SL, Watanabe M, Xu B, et al. (2007). Cited2, a coactivator of HNF4α, is essential for liver development. *EMBO J* **26**, 4445–4456.
[31] Novitskaya T, Baserga M, and de Caestecker MP (2011). Organ-specific defects in insulin-like growth factor and insulin receptor signaling in late gestational asymmetric intrauterine growth restriction in Cited1 mutant mice. *Endocrinology* **152**, 2503–2516.
[32] Teo JL and Kahn M (2010). The Wnt signaling pathway in cellular proliferation and differentiation: a tale of two coactivators. *Adv Drug Deliv Rev* **62**, 1149–1155.
[33] Yahata T, de Caestecker MP, Lechleider RJ, Andriole S, Roberts AB, Isselbacher KJ, and Shioda T (2000). The MSG1 non-DNA-binding transactivator binds to the p300/CBP coactivators, enhancing their functional link to the Smad transcription factors. *J Biol Chem* **275**, 8825–8834.
[34] Koch A, Waha A, Hartmann W, Hrychyk A, Schuller U, Wharton KA Jr, Fuchs SY, von Schweinitz D, and Pietsch T (2005). Elevated expression of Wnt antagonists is a common event in hepatoblastomas. *Clin Cancer Res* **11**, 4295–4304.

Table W1. Primer Sequences.

Gene	Primer Sequence or Catalog Number (for TaqMan Assays)
qRT-PCR primer sequences	
CITED1	Forward primer, 5′-AGGATGCCAACCAAGAGATG-3′
	Reverse primer, 5′-TGGTTCCATTTGAGGCTACC-3′
CXXC4	Forward primer, 5′-CAACCCAGCCAAGAAGAAGA-3′
	Reverse primer, 5′-AGATCTGGTGTCCCGTTTTG-3′
DKK1	Forward primer, 5′-TCCGAGGAGAAATTGAGGAA-3′
	Reverse primer, 5′-CCACAGTAACAACGCTGGAA-3′
*KREMEN1**	Hs00230750_m1 (spans exons 2–3 junction)
*PCNA**	Hs00427214_g1 (spans exons 3–4 junction)
*GAPDH**	Hs99999905_m1 (spans exons 3–4 junction)
cDNA sequencing primers for detection of CTNNB1 mutations	
CTNNB1	Forward primer (exons 2–4), 5′-AAAATCCAGCGTGGACAATGG-3′
	Reverse primer (exons 2–4), 5′-TGTGGCAAGTTCTGCATCATC-3′
	Forward primer (exons 1–5), 5′-GGAGGAAGGTCTGAGGAGCAG-3′
	Reverse primer (exons 1–5), 5′-CGATGATGGGAAGGTTATGC-3′

*TaqMan probe–based gene expression analysis assays from Applied Biosystems. Sequences are proprietary, but exon-exon boundaries to which primers and probe are designed are listed.

Table W2a. Gene List for Wnt Pathway RT^2 PCR Array.

Position	Unigene	Refseq	Symbol	Description
A01	Hs.515053	NM_001130	AES	Amino-terminal enhancer of split
A02	Hs.158932	NM_000038	APC	Adenomatous polyposis coli
A03	Hs.592082	NM_003502	AXIN1	Axin 1
A04	Hs.415209	NM_004326	BCL9	B cell CLL/lymphoma 9
A05	Hs.643802	NM_033637	BTRC	β-Transducin repeat containing
A06	Hs.17631	NM_003468	FZD5	Frizzled family receptor 5
A07	Hs.523852	NM_053056	CCND1	Cyclin D1
A08	Hs.376071	NM_001759	CCND2	Cyclin D2
A09	Hs.534307	NM_001760	CCND3	Cyclin D3
A10	Hs.529862	NM_001892	CSNK1A1	Casein kinase 1, α1
A11	Hs.631725	NM_001893	CSNK1D	Casein kinase 1, Δ
A12	Hs.646508	NM_022048	CSNK1G1	Casein kinase 1, γ1
B01	Hs.644056	NM_001895	CSNK2A1	Casein kinase 2, α1 polypeptide
B02	Hs.208597	NM_001328	CTBP1	C-terminal binding protein 1
B03	Hs.501345	NM_022802	CTBP2	C-terminal binding protein 2
B04	Hs.476018	NM_001904	CTNNB1	Catenin (cadherin-associated protein), β1, 88 kDa
B05	Hs.463759	NM_020248	CTNNBIP1	Catenin, β interacting protein 1
B06	Hs.12248	NM_025212	CXXC4	CXXC4
B07	Hs.654934	NM_014992	DAAM1	Dishevelled associated activator of morphogenesis 1
B08	Hs.655626	NM_033425	DIXDC1	DIX domain containing 1
B09	Hs.40499	NM_012242	DKK1	Dickkopf homolog 1 (*Xenopus laevis*)
B10	Hs.74375	NM_004421	DVL1	Dishevelled, dsh homolog 1 (*Drosophila*)
B11	Hs.118640	NM_004422	DVL2	Dishevelled, dsh homolog 2 (*Drosophila*)
B12	Hs.517517	NM_001429	EP300	E1A binding protein p300
C01	Hs.484138	NM_012300	FBXW11	F-box and WD repeat domain containing 11
C02	Hs.494985	NM_012164	FBXW2	F-box and WD repeat domain containing 2
C03	Hs.1755	NM_002007	FGF4	Fibroblast growth factor 4
C04	Hs.283565	NM_005438	FOSL1	FOS-like antigen 1
C05	Hs.663679	NM_003593	FOXN1	Forkhead box N1
C06	Hs.126057	NM_005479	FRAT1	Frequently rearranged in advanced T cell lymphomas
C07	Hs.128453	NM_001463	FRZB	Frizzled-related protein
C08	Hs.36975	NM_000510	FSHB	Follicle stimulating hormone, β polypeptide
C09	Hs.94234	NM_003505	FZD1	Frizzled family receptor 1
C10	Hs.142912	NM_001466	FZD2	Frizzled family receptor 2
C11	Hs.40735	NM_017412	FZD3	Frizzled family receptor 3
C12	Hs.19545	NM_012193	FZD4	Frizzled family receptor 4
D01	Hs.591863	NM_003506	FZD6	Frizzled family receptor 6
D02	Hs.173859	NM_003507	FZD7	Frizzled family receptor 7
D03	Hs.302634	NM_031866	FZD8	Frizzled family receptor 8
D04	Hs.466828	NM_019884	GSK3A	Glycogen synthase kinase 3α
D05	Hs.445733	NM_002093	GSK3B	Glycogen synthase kinase 3β
D06	Hs.714791	NM_002228	JUN	Jun proto-oncogene
D07	Hs.229335	NM_001039570	KREMEN1	Kringle containing transmembrane protein 1
D08	Hs.555947	NM_016269	LEF1	Lymphoid enhancer-binding factor 1
D09	Hs.6347	NM_002335	LRP5	Low density lipoprotein receptor-related protein 5
D10	Hs.584775	NM_002336	LRP6	Low density lipoprotein receptor-related protein 6
D11	Hs.202453	NM_002467	MYC	V-myc myelocytomatosis viral oncogene homolog (avian)
D12	Hs.592059	NM_033119	NKD1	Naked cuticle homolog 1 (*Drosophila*)

Table W2a. (*continued*)

Position	Unigene	Refseq	Symbol	Description
E01	Hs.208759	NM_016231	NLK	Nemo-like kinase
E02	Hs.643588	NM_000325	PITX2	Paired-like homeodomain 2
E03	Hs.386453	NM_022825	PORCN	Porcupine homolog (*Drosophila*)
E04	Hs.483408	NM_002715	PPP2CA	Protein phosphatase 2, catalytic subunit, α isozyme
E05	Hs.467192	NM_014225	PPP2R1A	Protein phosphatase 2, regulatory subunit A, α
E06	Hs.256587	NM_015617	PYGO1	Pygopus homolog 1 (*Drosophila*)
E07	Hs.647774	NM_021205	RHOU	Ras homolog gene family, member U
E08	Hs.401388	NM_021627	SENP2	SUMO1/sentrin/SMT3 specific peptidase 2
E09	Hs.713546	NM_003012	SFRP1	Secreted frizzled-related protein 1
E10	Hs.658169	NM_003014	SFRP4	Secreted frizzled-related protein 4
E11	Hs.500822	NM_022039	FBXW4	F-box and WD repeat domain containing 4
E12	Hs.728760	NM_004252	SLC9A3R1	Solute carrier family 9 (sodium/hydrogen exchanger), member 3 regulator 1
F01	Hs.98367	NM_022454	SOX17	SRY (sex determining region Y)–box 17
F02	Hs.389457	NM_003181	T	T, brachyury homolog (mouse)
F03	Hs.573153	NM_003202	TCF7	Transcription factor 7 (T cell specific, HMG box)
F04	Hs.516297	NM_031283	TCF7L1	Transcription factor 7–like 1 (T cell–specific, HMG box)
F05	Hs.197320	NM_005077	TLE1	Transducin-like enhancer of split 1 (E(sp1) homolog, *Drosophila*)
F06	Hs.332173	NM_003260	TLE2	Transducin-like enhancer of split 2 (E(sp1) homolog, *Drosophila*)
F07	Hs.284122	NM_007191	WIF1	WNT inhibitory factor 1
F08	Hs.492974	NM_003882	WISP1	WNT1 inducible signaling pathway protein 1
F09	Hs.248164	NM_005430	WNT1	Wingless-type MMTV integration site family, member 1
F10	Hs.121540	NM_025216	WNT10A	Wingless-type MMTV integration site family, member 10A
F11	Hs.108219	NM_004626	WNT11	Wingless-type MMTV integration site family, member 11
F12	Hs.272375	NM_057168	WNT16	Wingless-type MMTV integration site family, member 16
G01	Hs.567356	NM_003391	WNT2	Wingless-type MMTV integration site family member 2
G02	Hs.258575	NM_004185	WNT2B	Wingless-type MMTV integration site family, member 2B
G03	Hs.445884	NM_030753	WNT3	Wingless-type MMTV integration site family, member 3
G04	Hs.336930	NM_033131	WNT3A	Wingless-type MMTV integration site family, member 3A
G05	Hs.25766	NM_030761	WNT4	Wingless-type MMTV integration site family, member 4
G06	Hs.696364	NM_003392	WNT5A	Wingless-type MMTV integration site family, member 5A
G07	Hs.306051	NM_032642	WNT5B	Wingless-type MMTV integration site family, member 5B
G08	Hs.29764	NM_006522	WNT6	Wingless-type MMTV integration site family, member 6
G09	Hs.72290	NM_004625	WNT7A	Wingless-type MMTV integration site family, member 7A
G10	Hs.512714	NM_058238	WNT7B	Wingless-type MMTV integration site family, member 7B
G11	Hs.591274	NM_058244	WNT8A	Wingless-type MMTV integration site family, member 8A
G12	Hs.149504	NM_003395	WNT9A	Wingless-type MMTV integration site family, member 9A
H01	Hs.534255	NM_004048	B2M	β-2-microglobulin
H02	Hs.412707	NM_000194	HPRT1	Hypoxanthine phosphoribosyltransferase 1
H03	Hs.728776	NM_012423	RPL13A	Ribosomal protein L13a
H04	Hs.592355	NM_002046	GAPDH	Glyceraldehyde-3-phosphate dehydrogenase
H05	Hs.520640	NM_001101	ACTB	Actin, β
H06	N/A	SA_00105	HGDC	Human genomic DNA contamination
H07	N/A	SA_00104	RTC	RT control
H08	N/A	SA_00104	RTC	RT control
H09	N/A	SA_00104	RTC	RT control
H10	N/A	SA_00103	PPC	Positive PCR control
H11	N/A	SA_00103	PPC	Positive PCR control
H12	N/A	SA_00103	PPC	Positive PCR control

Table W2b. Average C_t.

		Average C_t		SD	
		Control Group	Group 1	Control Group	Group 1
A01	AES	24.35	24.48	0.645497	0.320156
A02	APC	30.4	30.45	0.774597	0.911043
A03	AXIN1	25.43	26.28	0.464579	0.330404
A04	BCL9	26.88	27.38	0.780491	0.512348
A05	BTRC	26.88	26.43	0.727438	0.670199
A06	FZD5	23.85	23.65	0.675771	0.6245
A07	CCND1	24.98	25.4	0.556028	0.804156
A08	CCND2	34.88	34.25	0.25	0.818535
A09	CCND3	28.4	28.7	0.316228	0.547723
A10	CSNK1A1	23.7	23.38	1.089342	0.434933
A11	CSNK1D	23.15	23.35	0.718795	0.173205
A12	CSNK1G1	31.23	31.2	0.377492	0.812404
B01	CSNK2A1	23.65	23.85	0.443471	0.310913
B02	CTBP1	22.7	23.08	0.522813	0.457347
B03	CTBP2	28.75	28.88	0.932738	1.212092
B04	CTNNB1	22.13	22.28	0.639661	0.492443
B05	CTNNBIP1	27.58	28.53	1.212092	0.623832
B06	CXXC4	32.38	30.9	1.078193	0.616441
B07	DAAM1	25.45	25.93	1.008299	0.655108
B08	DIXDC1	27.03	27.48	0.644851	0.670199
B09	DKK1	20.75	21.65	0.81035	1.567376
B10	DVL1	24.9	24.75	0.571548	0.5
B11	DVL2	29.33	29.1	0.411299	0.469042
B12	EP300	24.95	24.9	0.925563	0.739369
C01	FBXW11	25.93	25.95	0.579511	0.288675
C02	FBXW2	28.7	28.8	0.503322	0.707107
C03	FGF4	35	35	0	0
C04	FOSL1	29.25	29.25	0.404145	0.412311
C05	FOXN1	33.7	34.78	1.536229	0.45
C06	FRAT1	28.75	28.65	0.785281	0.723418
C07	FRZB	28.13	31.2	1.007886	4.436215
C08	FSHB	34.93	35	0.15	0
C09	FZD1	30.3	30.1	0.909212	1.042433
C10	FZD2	35	35	0	0
C11	FZD3	27.48	27.53	0.85	0.221736
C12	FZD4	26.73	27.5	0.780491	0.983192
D01	FZD6	25.23	25.13	0.607591	0.442531
D02	FZD7	27.38	27.3	0.639661	0.469042
D03	FZD8	33.15	33.5	0.714143	0.57735
D04	GSK3A	25.78	26.08	0.464579	0.298608
D05	GSK3B	23.6	23.6	0.716473	0.559762
D06	JUN	26.4	26.35	0.752773	0.704746
D07	KREMEN1	28.73	28.1	0.531507	0.216025
D08	LEF1	25.23	25.43	0.499166	0.680074
D09	LRP5	25.68	25.93	0.330404	0.262996
D10	LRP6	24.75	24.68	0.750555	0.567891
D11	MYC	25.33	25.73	0.629153	0.30957
D12	NKD1	23.8	23.7	0.326599	0.469042

Table W2b. (*continued*)

		Average C_t		SD	
		Control Group	Group 1	Control Group	Group 1
E01	NLK	26.3	26.2	0.668331	0.588784
E02	PITX2	28.1	27.83	0.983192	0.780491
E03	PORCN	27.9	28.18	0.559762	0.320156
E04	PPP2CA	26.7	26.83	0.432049	0.531507
E05	PPP2R1A	22.23	22.48	0.411299	0.320156
E06	PYGO1	28	28	0.535413	0.374166
E07	RHOU	23.78	24.18	0.537742	0.377492
E08	SENP2	25.2	25.48	0.496655	0.4272
E09	SFRP1	34.7	35	0.6	0
E10	SFRP4	29.83	30.58	0.914239	0.618466
E11	FBXW4	25.85	25.83	0.704746	0.585235
E12	SLC9A3R1	21.15	21.43	0.420317	0.35
F01	SOX17	35	35	0	0
F02	T	33.4	33.45	1.202775	0.619139
F03	TCF7	30.5	30.73	0.535413	0.377492
F04	TCF7L1	29.33	28.83	0.846069	0.287228
F05	TLE1	24.95	24.8	0.544671	0.648074
F06	TLE2	34.68	34.9	0.65	0.2
F07	WIF1	34.6	35	0.8	0
F08	WISP1	35	35	0	0
F09	WNT1	34.43	35	1.15	0
F10	WNT10A	32.65	33.53	2.977135	1.839157
F11	WNT11	30.58	32.03	0.411299	2.075853
F12	WNT16	34.2	33.75	1.28841	1.452584
G01	WNT2	35	35	0	0
G02	WNT2B	30.68	30.68	0.899537	1.652019
G03	WNT3	27.23	27.45	0.75	0.479583
G04	WNT3A	35	35	0	0
G05	WNT4	32.85	33.73	1.3	0.895824
G06	WNT5A	29.13	29.43	0.809835	0.537742
G07	WNT5B	34.73	35	0.377492	0
G08	WNT6	35	34.83	0	0.35
G09	WNT7A	35	35	0	0
G10	WNT7B	35	35	0	0
G11	WNT8A	35	34.95	0	0.1
G12	WNT9A	35	35	0	0
H01	B2M	21.05	21.55	0.519615	0.404145
H02	HPRT1	24.35	24.7	0.550757	0.637704
H03	RPL13A	19.73	19.55	0.55	0.369685
H04	GAPDH	16.58	16.65	0.660177	0.532291
H05	ACTB	19.13	18.95	0.655108	0.568624
H06	HGDC	35	35	0	0
H07	RTC	21.93	22.83	0.359398	0.330404
H08	RTC	22.43	23.4	0.368556	0.294392
H09	RTC	22.15	23.08	0.387298	0.499166
H10	PPC	18.65	19.23	0.493288	0.298608
H11	PPC	18.58	19.08	0.457347	0.330404
H12	PPC	18.3	18.78	0.391578	0.262996

Table W2c. Average ΔC_t.

		Average ΔC_t [C_t (GOI) – Average C_t (HKG)]		SD	
		Control Group	Group 1	Control Group	Group 1
A01	AES	4.383333	4.458333	0.551429	0.464579
A02	APC	10.433333	10.433333	0.438009	0.514242
A03	AXIN1	5.458333	6.258333	0.574376	0.512348
A04	BCL9	6.908333	7.358333	0.448351	0.403113
A05	BTRC	6.908333	6.408333	0.593405	0.481029
A06	FZD5	3.883333	3.633333	0.475706	0.316228
A07	CCND1	5.008333	5.383333	0.242479	0.404145
A08	CCND2	14.908333	14.233333	0.460575	0.684755
A09	CCND3	8.433333	8.683333	0.222777	0.31798
A10	CSNK1A1	3.733333	3.358333	0.833111	0.485627
A11	CSNK1D	3.183333	3.333333	0.439275	0.253859
A12	CSNK1G1	11.258333	11.183333	0.260164	0.420317
B01	CSNK2A1	3.683333	3.833333	0.244192	0.124722
B02	CTBP1	2.733333	3.058333	0.479197	0.514512
B03	CTBP2	8.783333	8.858333	0.684484	0.899537
B04	CTNNB1	2.158333	2.258333	0.341429	0.452462
B05	CTNNBIP1	7.608333	8.508333	1.0847	0.594652
B06	CXXC4	12.408333	10.883333	0.869813	0.738617
B07	DAAM1	5.483333	5.908333	0.654613	0.262996
B08	DIXDC1	7.058333	7.458333	0.412198	0.492443
B09	DKK1	0.783333	1.633333	0.630403	1.61314
B10	DVL1	4.933333	4.733333	0.448041	0.221108
B11	DVL2	9.358333	9.083333	0.21322	0.088192
B12	EP300	4.983333	4.883333	0.684484	0.574456
C01	FBXW11	5.958333	5.933333	0.490936	0.226078
C02	FBXW2	8.733333	8.783333	0.136083	0.440959
C03	FGF4	15.033333	14.983333	0.372181	0.412311
C04	FOSL1	9.283333	9.233333	0.19341	0.377124
C05	FOXN1	13.733333	14.758333	1.243948	0.471699
C06	FRAT1	8.783333	8.633333	0.664719	0.694422
C07	FRZB	8.158333	11.183333	0.678983	4.205948
C08	FSHB	14.958333	14.983333	0.409494	0.412311
C09	FZD1	10.333333	10.083333	0.822372	1.173314
C10	FZD2	15.033333	14.983333	0.372181	0.412311
C11	FZD3	7.508333	7.508333	0.578232	0.432371
C12	FZD4	6.758333	7.483333	0.525903	0.635085
D01	FZD6	5.258333	5.108333	0.438326	0.313138
D02	FZD7	7.408333	7.283333	0.56462	0.552771
D03	FZD8	13.183333	13.483333	1.027222	0.724952
D04	GSK3A	5.808333	6.058333	0.247019	0.287228
D05	GSK3B	3.633333	3.583333	0.445554	0.218581
D06	JUN	6.433333	6.333333	0.476873	0.454606
D07	KREMEN1	8.758333	8.083333	0.344668	0.338296
D08	LEF1	5.258333	5.408333	0.27672	0.718215
D09	LRP5	5.708333	5.908333	0.172938	0.195078
D10	LRP6	4.783333	4.658333	0.482662	0.211476
D11	MYC	5.358333	5.708333	0.568543	0.413991
D12	NKD1	3.833333	3.683333	0.306715	0.247207

Table W2c. (*continued*)

		Average ΔC_t [C_t (GOI) – Average C_t (HKG)]		SD	
		Control Group	Group 1	Control Group	Group 1
E01	NLK	6.333333	6.183333	0.52985	0.422953
E02	PITX2	8.133333	7.808333	0.894841	0.822091
E03	PORCN	7.933333	8.158333	0.552436	0.330404
E04	PPP2CA	6.733333	6.808333	0.098131	0.183333
E05	PPP2R1A	2.258333	2.458333	0.303529	0.397562
E06	PYGO1	8.033333	7.983333	0.306715	0.310913
E07	RHOU	3.808333	4.158333	0.378472	0.183333
E08	SENP2	5.233333	5.458333	0.476873	0.254406
E09	SFRP1	14.733333	14.983333	0.313877	0.412311
E10	SFRP4	9.858333	10.558333	0.655673	0.206155
E11	FBXW4	5.883333	5.808333	0.599691	0.476387
E12	SLC9A3R1	1.183333	1.408333	0.270117	0.294863
F01	SOX17	15.033333	14.983333	0.372181	0.412311
F02	T	13.433333	13.433333	0.855483	0.507718
F03	TCF7	10.533333	10.708333	0.320878	0.705731
F04	TCF7L1	9.358333	8.808333	0.572438	0.236291
F05	TLE1	4.983333	4.783333	0.345875	0.425572
F06	TLE2	14.708333	14.883333	0.357331	0.378594
F07	WIF1	14.633333	14.983333	0.495162	0.412311
F08	WISP1	15.033333	14.983333	0.372181	0.412311
F09	WNT1	14.458333	14.983333	0.833278	0.412311
F10	WNT10A	12.683333	13.508333	2.646941	1.631717
F11	WNT11	10.608333	12.008333	0.395694	1.678044
F12	WNT16	14.233333	13.733333	1.015801	1.244544
G01	WNT2	15.033333	14.983333	0.372181	0.412311
G02	WNT2B	10.708333	10.658333	0.699934	1.279865
G03	WNT3	7.258333	7.433333	0.606371	0.418994
G04	WNT3A	15.033333	14.983333	0.372181	0.412311
G05	WNT4	12.883333	13.708333	1.143905	0.820738
G06	WNT5A	9.158333	9.408333	0.554694	0.305959
G07	WNT5B	14.758333	14.983333	0.707827	0.412311
G08	WNT6	15.033333	14.808333	0.372181	0.419325
G09	WNT7A	15.033333	14.983333	0.372181	0.412311
G10	WNT7B	15.033333	14.983333	0.372181	0.412311
G11	WNT8A	15.033333	14.933333	0.372181	0.394405
G12	WNT9A	15.033333	14.983333	0.372181	0.412311
H01	B2M	1.083333	1.533333	0.402308	0.169967
H02	HPRT1	4.383333	4.683333	0.361581	0.51099
H03	RPL13A	−0.241667	−0.466667	0.242479	0.235702
H04	GAPDH	−3.391667	−3.366667	0.29234	0.323179
H05	ACTB	−0.841667	−1.066667	0.604535	0.169967
H06	HGDC	15.033333	14.983333	0.372181	0.412311
H07	RTC	1.958333	2.808333	0.602695	0.56001
H08	RTC	2.458333	3.383333	0.598996	0.465475
H09	RTC	2.183333	3.058333	0.586578	0.700991
H10	PPC	−1.316667	−0.791667	0.355382	0.471699
H11	PPC	−1.391667	−0.941667	0.21322	0.533594
H12	PPC	−1.666667	−1.241667	0.237268	0.485627

Table W2d. $2^{-\text{Average}(\Delta Ct)}$.

		$2^{-\text{Average}(\Delta Ct)}$	
		Control Group	Group 1
A01	AES	0.047917	0.045489
A02	APC	0.000723	0.000723
A03	AXIN1	0.022745	0.013063
A04	BCL9	0.008325	0.006094
A05	BTRC	0.008325	0.011773
A06	FZD5	0.067764	0.080586
A07	CCND1	0.03107	0.023958
A08	CCND2	0.000033	0.000052
A09	CCND3	0.002893	0.002433
A10	CSNK1A1	0.075189	0.097508
A11	CSNK1D	0.110083	0.099213
A12	CSNK1G1	0.000408	0.00043
B01	CSNK2A1	0.077841	0.070154
B02	CTBP1	0.150378	0.120047
B03	CTBP2	0.00227	0.002155
B04	CTNNB1	0.224015	0.209013
B05	CTNNBIP1	0.005125	0.002746
B06	CXXC4	0.000184	0.000529
B07	DAAM1	0.022354	0.01665
B08	DIXDC1	0.007503	0.005686
B09	DKK1	0.581023	0.322343
B10	DVL1	0.032728	0.037595
B11	DVL2	0.001524	0.001844
B12	EP300	0.031613	0.033882
C01	FBXW11	0.016083	0.016364
C02	FBXW2	0.00235	0.00227
C03	FGF4	0.00003	0.000031
C04	FOSL1	0.001605	0.001661
C05	FOXN1	0.000073	0.000036
C06	FRAT1	0.00227	0.002518
C07	FRZB	0.0035	0.00043
C08	FSHB	0.000031	0.000031
C09	FZD1	0.000775	0.000922
C10	FZD2	0.00003	0.000031
C11	FZD3	0.005492	0.005492
C12	FZD4	0.009237	0.005588
D01	FZD6	0.026127	0.028989
D02	FZD7	0.005887	0.006419
D03	FZD8	0.000108	0.000087
D04	GSK3A	0.017845	0.015006
D05	GSK3B	0.080586	0.083427
D06	JUN	0.011571	0.012402
D07	KREMEN1	0.002309	0.003687
D08	LEF1	0.026127	0.023547
D09	LRP5	0.019126	0.01665
D10	LRP6	0.036314	0.039601
D11	MYC	0.024377	0.019126
D12	NKD1	0.070154	0.077841

Table W2d. (*continued*)

		$2^{-\text{Average}(\Delta Ct)}$	
		Control Group	Group 1
E01	NLK	0.012402	0.01376
E02	PITX2	0.003561	0.004461
E03	PORCN	0.004091	0.0035
E04	PPP2CA	0.009399	0.008923
E05	PPP2R1A	0.209013	0.181957
E06	PYGO1	0.003817	0.003952
E07	RHOU	0.07138	0.056004
E08	SENP2	0.026583	0.022745
E09	SFRP1	0.000037	0.000031
E10	SFRP4	0.001077	0.000663
E11	FBXW4	0.016941	0.017845
E12	SLC9A3R1	0.440333	0.376747
F01	SOX17	0.00003	0.000031
F02	T	0.00009	0.00009
F03	TCF7	0.000675	0.000598
F04	TCF7L1	0.001524	0.002231
F05	TLE1	0.031613	0.036314
F06	TLE2	0.000037	0.000033
F07	WIF1	0.000039	0.000031
F08	WISP1	0.00003	0.000031
F09	WNT1	0.000044	0.000031
F10	WNT10A	0.000152	0.000086
F11	WNT11	0.000641	0.000243
F12	WNT16	0.000052	0.000073
G01	WNT2	0.00003	0.000031
G02	WNT2B	0.000598	0.000619
G03	WNT3	0.006532	0.005786
G04	WNT3A	0.00003	0.000031
G05	WNT4	0.000132	0.000075
G06	WNT5A	0.00175	0.001472
G07	WNT5B	0.000036	0.000031
G08	WNT6	0.00003	0.000035
G09	WNT7A	0.00003	0.000031
G10	WNT7B	0.00003	0.000031
G11	WNT8A	0.00003	0.000032
G12	WNT9A	0.00003	0.000031
H01	B2M	0.471937	0.345478
H02	HPRT1	0.047917	0.03892
H03	RPL13A	1.182358	1.381913
H04	GAPDH	10.495265	10.314962
H05	ACTB	1.792119	2.094588
H06	HGDC	0.00003	0.000031
H07	RTC	0.257326	0.14276
H08	RTC	0.181957	0.095833
H09	RTC	0.220166	0.120047
H10	PPC	2.490899	1.731073
H11	PPC	2.623816	1.920746
H12	PPC	3.174802	2.364716

Table W2e. Fold Change.

		Fold Change (Compared to Control Group)		
		Group 1		
		Fold Change	95% CI	Comments
A01	AES	0.9493	(0.48, 1.41)	Okay
A02	APC	1	(0.54, 1.46)	B
A03	AXIN1	0.5743	(0.27, 0.87)	Okay
A04	BCL9	0.732	(0.43, 1.03)	Okay
A05	BTRC	1.4142	(0.68, 2.15)	Okay
A06	FZD5	1.1892	(0.73, 1.65)	Okay
A07	CCND1	0.7711	(0.52, 1.02)	Okay
A08	CCND2	1.5966	(0.70, 2.49)	B
A09	CCND3	0.8409	(0.62, 1.06)	Okay
A10	CSNK1A1	1.2968	(0.45, 2.15)	Okay
A11	CSNK1D	0.9013	(0.59, 1.21)	Okay
A12	CSNK1G1	1.0534	(0.70, 1.41)	B
B01	CSNK2A1	0.9013	(0.73, 1.07)	Okay
B02	CTBP1	0.7983	(0.42, 1.18)	Okay
B03	CTBP2	0.9493	(0.22, 1.68)	Okay
B04	CTNNB1	0.933	(0.57, 1.29)	Okay
B05	CTNNBIP1	0.5359	(0.09, 0.99)	Okay
B06	CXXC4	2.8779	(0.65, 5.11)	Okay
B07	DAAM1	0.7448	(0.39, 1.10)	Okay
B08	DIXDC1	0.7579	(0.43, 1.09)	Okay
B09	DKK1	0.5548	(0.00001, 1.21)	Okay
B10	DVL1	1.1487	(0.76, 1.54)	Okay
B11	DVL2	1.21	(1.02, 1.40)	Okay
B12	EP300	1.0718	(0.42, 1.72)	Okay
C01	FBXW11	1.0175	(0.64, 1.39)	Okay
C02	FBXW2	0.9659	(0.66, 1.27)	Okay
C03	FGF4	1.0353	(0.64, 1.43)	C
C04	FOSL1	1.0353	(0.74, 1.33)	Okay
C05	FOXN1	0.4914	(0.05, 0.94)	B
C06	FRAT1	1.1096	(0.39, 1.83)	Okay
C07	FRZB	0.1229	(0.00001, 0.48)	A
C08	FSHB	0.9828	(0.59, 1.37)	B
C09	FZD1	1.1892	(0.03, 2.35)	B
C10	FZD2	1.0353	(0.64, 1.43)	C
C11	FZD3	1	(0.51, 1.49)	Okay
C12	FZD4	0.605	(0.27, 0.94)	Okay
D01	FZD6	1.1096	(0.70, 1.52)	Okay
D02	FZD7	1.0905	(0.51, 1.68)	Okay
D03	FZD8	0.8123	(0.12, 1.51)	B
D04	GSK3A	0.8409	(0.62, 1.06)	Okay
D05	GSK3B	1.0353	(0.69, 1.38)	Okay
D06	JUN	1.0718	(0.59, 1.55)	Okay
D07	KREMEN1	1.5966	(1.07, 2.12)	Okay
D08	LEF1	0.9013	(0.43, 1.37)	Okay
D09	LRP5	0.8706	(0.72, 1.02)	Okay
D10	LRP6	1.0905	(0.70, 1.48)	Okay
D11	MYC	0.7846	(0.41, 1.16)	Okay
D12	NKD1	1.1096	(0.81, 1.41)	Okay
E01	NLK	1.1096	(0.60, 1.62)	Okay
E02	PITX2	1.2527	(0.22, 2.29)	Okay
E03	PORCN	0.8556	(0.48, 1.23)	Okay
E04	PPP2CA	0.9493	(0.82, 1.08)	Okay
E05	PPP2R1A	0.8706	(0.57, 1.17)	Okay
E06	PYGO1	1.0353	(0.73, 1.34)	Okay
E07	RHOU	0.7846	(0.56, 1.01)	Okay
E08	SENP2	0.8556	(0.54, 1.17)	Okay
E09	SFRP1	0.8409	(0.54, 1.14)	B
E10	SFRP4	0.6156	(0.33, 0.90)	A
E11	FBXW4	1.0534	(0.51, 1.60)	Okay
E12	SLC9A3R1	0.8556	(0.62, 1.09)	Okay
F01	SOX17	1.0353	(0.64, 1.43)	C
F02	T	1	(0.32, 1.68)	B
F03	TCF7	0.8858	(0.42, 1.35)	B
F04	TCF7L1	1.4641	(0.85, 2.08)	Okay
F05	TLE1	1.1487	(0.72, 1.58)	Okay
F06	TLE2	0.8858	(0.57, 1.20)	B
F07	WIF1	0.7846	(0.44, 1.13)	B
F08	WISP1	1.0353	(0.64, 1.43)	C
F09	WNT1	0.695	(0.26, 1.13)	B
F10	WNT10A	0.5645	(0.00001, 1.76)	B
F11	WNT11	0.3789	(0.00001, 0.82)	B
F12	WNT16	1.4142	(0.00001, 2.96)	B
G01	WNT2	1.0353	(0.64, 1.43)	C
G02	WNT2B	1.0353	(0.01, 2.06)	B
G03	WNT3	0.8858	(0.44, 1.33)	Okay
G04	WNT3A	1.0353	(0.64, 1.43)	C
G05	WNT4	0.5645	(0.02, 1.10)	B
G06	WNT5A	0.8409	(0.48, 1.20)	Okay
G07	WNT5B	0.8556	(0.38, 1.33)	B
G08	WNT6	1.1688	(0.72, 1.61)	B
G09	WNT7A	1.0353	(0.64, 1.43)	C
G10	WNT7B	1.0353	(0.64, 1.43)	C
G11	WNT8A	1.0718	(0.68, 1.47)	B
G12	WNT9A	1.0353	(0.64, 1.43)	C
H01	B2M	0.732	(0.51, 0.95)	Okay
H02	HPRT1	0.8123	(0.47, 1.16)	Okay
H03	RPL13A	1.1688	(0.90, 1.44)	Okay
H04	GAPDH	0.9828	(0.69, 1.27)	Okay
H05	ACTB	1.1688	(0.67, 1.67)	Okay
H06	HGDC	1.0353	(0.64, 1.43)	C
H07	RTC	0.5548	(0.24, 0.86)	Okay
H08	RTC	0.5267	(0.26, 0.80)	Okay
H09	RTC	0.5453	(0.21, 0.88)	Okay
H10	PPC	0.695	(0.42, 0.97)	Okay
H11	PPC	0.732	(0.45, 1.02)	Okay
H12	PPC	0.7448	(0.47, 1.02)	Okay

Table W2e. (*continued*)

Comments:

A: This gene's average threshold cycle is relatively high (>30) in either the control or the test sample and is reasonably low in the other sample (<30).

These data mean that the gene's expression is relatively low in one sample and reasonably detected in the other sample, suggesting that the actual fold-change value is at least as large as the calculated and reported fold-change result.

This fold-change result may also have greater variations if $P > .05$; therefore, it is important to have a sufficient number of biologic replicates to validate the result for this gene.

B: This gene's average threshold cycle is relatively high (>30), meaning that its relative expression level is low, in both control and test samples, and the *P* value for the fold change is either unavailable or relatively high ($P > .05$).

This fold-change result may also have greater variations; therefore, it is important to have a sufficient number of biologic replicates to validate the result for this gene.

C: This gene's average threshold cycle is either not determined or greater than the defined cutoff value (default 35), in both samples meaning that its expression was undetected, making this fold-change result erroneous and uninterpretable.

Fold change and fold regulation:

Fold change ($2^{-\Delta\Delta Ct}$) is the normalized gene expression ($2^{-\Delta Ct}$) in the test sample divided by the normalized gene expression ($2^{-\Delta Ct}$) in the control sample.

Fold regulation represents fold-change results in a biologically meaningful way. Fold-change values greater than 1 indicate a positive or an up-regulation, and the fold regulation is equal to the fold change. Fold-change values less than 1 indicate a negative or down-regulation, and the fold regulation is the negative inverse of the fold change.

Fold-change and fold-regulation values greater than 2 are indicated in red; fold-change values less than 0.5 and fold-regulation values less than –2 are indicated in blue.

Table W2f. *P* values.

		P Value (Compared to Control Group)
		Group 1
A01	AES	0.792341
A02	APC	0.965095
A03	AXIN1	0.125466
A04	BCL9	0.200823
A05	BTRC	0.198872
A06	FZD5	0.434184
A07	CCND1	0.1434
A08	CCND2	0.130908
A09	CCND3	0.26405
A10	CSNK1A1	0.581515
A11	CSNK1D	0.502102
A12	CSNK1G1	0.690156
B01	CSNK2A1	0.294784
B02	CTBP1	0.379823
B03	CTBP2	0.96217
B04	CTNNB1	0.757378
B05	CTNNBIP1	0.138199
B06	CXXC4	0.043045
B07	DAAM1	0.294942
B08	DIXDC1	0.291973
B09	DKK1	0.746279
B10	DVL1	0.490117
B11	DVL2	0.042473
B12	EP300	0.888903
C01	FBXW11	0.941277
C02	FBXW2	0.995686
C03	FGF4	0.836286
C04	FOSL1	0.714447
C05	FOXN1	0.156795
C06	FRAT1	0.689437
C07	FRZB	0.76046
C08	FSHB	0.954679
C09	FZD1	0.515336
C10	FZD2	0.836286
C11	FZD3	0.922969
C12	FZD4	0.135681
D01	FZD6	0.652247
D02	FZD7	0.769613
D03	FZD8	0.548591
D04	GSK3A	0.225384
D05	GSK3B	0.967886
D06	JUN	0.790172
D07	KREMEN1	0.033755
D08	LEF1	0.90179
D09	LRP5	0.181439
D10	LRP6	0.780073
D11	MYC	0.292486
D12	NKD1	0.506295
E01	NLK	0.693875
E02	PITX2	0.718265
E03	PORCN	0.416707
E04	PPP2CA	0.535224
E05	PPP2R1A	0.475922
E06	PYGO1	0.833288
E07	RHOU	0.114162
E08	SENP2	0.356227
E09	SFRP1	0.441863
E10	SFRP4	0.119764
E11	FBXW4	0.886316
E12	SLC9A3R1	0.288113
F01	SOX17	0.836286
F02	T	0.836247
F03	TCF7	0.879469
F04	TCF7L1	0.126211
F05	TLE1	0.461623
F06	TLE2	0.558308
F07	WIF1	0.357022
F08	WISP1	0.836286
F09	WNT1	0.333883
F10	WNT10A	0.398512
F11	WNT11	0.104759
F12	WNT16	0.495047
G01	WNT2	0.836286
G02	WNT2B	0.690109
G03	WNT3	0.545446
G04	WNT3A	0.836286
G05	WNT4	0.151461
G06	WNT5A	0.380818
G07	WNT5B	0.526959
G08	WNT6	0.428128
G09	WNT7A	0.836286
G10	WNT7B	0.836286
G11	WNT8A	0.713394
G12	WNT9A	0.836286
H01	B2M	0.07127
H02	HPRT1	0.439236
H03	RPL13A	0.214986
H04	GAPDH	0.937356
H05	ACTB	0.727042
H06	HGDC	0.836286
H07	RTC	0.102875
H08	RTC	0.089411
H09	RTC	0.115337
H10	PPC	0.124293
H11	PPC	0.171647
H12	PPC	0.184196

P value:
The *P* values are calculated based on a Student's *t* test of the replicate $2^{-\Delta Ct}$ values for each gene in the control group and treatment groups, and *P* values less than .05 are indicated in red.

Table W2g. Fold Regulation.

		Up-regulation/Down-regulation (Compared to Control Group)	
		Group 1	
		Fold Regulation	Comments
A01	AES	−1.0534	Okay
A02	APC	1	B
A03	AXIN1	−1.7411	Okay
A04	BCL9	−1.366	Okay
A05	BTRC	1.4142	Okay
A06	FZD5	1.1892	Okay
A07	CCND1	−1.2968	Okay
A08	CCND2	1.5966	B
A09	CCND3	−1.1892	Okay
A10	CSNK1A1	1.2968	Okay
A11	CSNK1D	−1.1096	Okay
A12	CSNK1G1	1.0534	B
B01	CSNK2A1	−1.1096	Okay
B02	CTBP1	−1.2527	Okay
B03	CTBP2	−1.0534	Okay
B04	CTNNB1	−1.0718	Okay
B05	CTNNBIP1	−1.8661	Okay
B06	CXXC4	2.8779	Okay
B07	DAAM1	−1.3426	Okay
B08	DIXDC1	−1.3195	Okay
B09	DKK1	−1.8025	Okay
B10	DVL1	1.1487	Okay
B11	DVL2	1.21	Okay
B12	EP300	1.0718	Okay
C01	FBXW11	1.0175	Okay
C02	FBXW2	−1.0353	Okay
C03	FGF4	1.0353	C
C04	FOSL1	1.0353	Okay
C05	FOXN1	−2.035	B
C06	FRAT1	1.1096	Okay
C07	FRZB	−8.1398	A
C08	FSHB	−1.0175	B
C09	FZD1	1.1892	B
C10	FZD2	1.0353	C
C11	FZD3	1	Okay
C12	FZD4	−1.6529	Okay
D01	FZD6	1.1096	Okay
D02	FZD7	1.0905	Okay
D03	FZD8	−1.2311	B
D04	GSK3A	−1.1892	Okay
D05	GSK3B	1.0353	Okay
D06	JUN	1.0718	Okay
D07	KREMEN1	1.5966	Okay
D08	LEF1	−1.1096	Okay
D09	LRP5	−1.1487	Okay
D10	LRP6	1.0905	Okay
D11	MYC	−1.2746	Okay
D12	NKD1	1.1096	Okay
E01	NLK	1.1096	Okay
E02	PITX2	1.2527	Okay
E03	PORCN	−1.1688	Okay
E04	PPP2CA	−1.0534	Okay
E05	PPP2R1A	−1.1487	Okay
E06	PYGO1	1.0353	Okay
E07	RHOU	−1.2746	Okay
E08	SENP2	−1.1688	Okay
E09	SFRP1	−1.1892	B
E10	SFRP4	−1.6245	A
E11	FBXW4	1.0534	Okay
E12	SLC9A3R1	−1.1688	Okay
F01	SOX17	1.0353	C
F02	T	1	B
F03	TCF7	−1.129	B
F04	TCF7L1	1.4641	Okay
F05	TLE1	1.1487	Okay
F06	TLE2	−1.129	B
F07	WIF1	−1.2746	B
F08	WISP1	1.0353	C
F09	WNT1	−1.4389	B
F10	WNT10A	−1.7715	B
F11	WNT11	−2.639	B
F12	WNT16	1.4142	B
G01	WNT2	1.0353	C
G02	WNT2B	1.0353	B
G03	WNT3	−1.129	Okay
G04	WNT3A	1.0353	C
G05	WNT4	−1.7715	B
G06	WNT5A	−1.1892	Okay
G07	WNT5B	−1.1688	B
G08	WNT6	1.1688	B
G09	WNT7A	1.0353	C
G10	WNT7B	1.0353	C
G11	WNT8A	1.0718	B
G12	WNT9A	1.0353	C
H01	B2M	−1.366	Okay
H02	HPRT1	−1.2311	Okay
H03	RPL13A	1.1688	Okay
H04	GAPDH	−1.0175	Okay
H05	ACTB	1.1688	Okay
H06	HGDC	1.0353	C
H07	RTC	−1.8025	Okay
H08	RTC	−1.8987	Okay
H09	RTC	−1.834	Okay
H10	PPC	−1.4389	Okay
H11	PPC	−1.366	Okay
H12	PPC	−1.3426	Okay

Table W2g. (*continued*)

Comments:

A: This gene's average threshold cycle is relatively high (>30) in either the control or the test sample and is reasonably low in the other sample (<30).

These data mean that the gene's expression is relatively low in one sample and reasonably detected in the other sample suggesting that the actual fold-change value is at least as large as the calculated and reported fold-change result.

This fold-change result may also have greater variations if $P > .05$; therefore, it is important to have a sufficient number of biologic replicates to validate the result for this gene.

B: This gene's average threshold cycle is relatively high (>30), meaning that its relative expression level is low, in both control and test samples, and the P value for the fold change is either unavailable or relatively high ($P > .05$).

This fold-change result may also have greater variations; therefore, it is important to have a sufficient number of biologic replicates to validate the result for this gene.

C: This gene's average threshold cycle is either not determined or greater than the defined cutoff value (default 35), in both samples meaning that its expression was undetected, making this fold-change result erroneous and uninterpretable.

Fold change and fold regulation:

Fold change ($2^{-\Delta\Delta Ct}$) is the normalized gene expression ($2^{-\Delta Ct}$) in the test sample divided by the normalized gene expression ($2^{-\Delta Ct}$) in the control sample.

Fold regulation represents fold-change results in a biologically meaningful way. Fold-change values greater than 1 indicate a positive or an up-regulation, and the fold regulation is equal to the fold change. Fold-change values less than 1 indicate a negative or down-regulation, and the fold regulation is the negative inverse of the fold change.

Fold-change and fold-regulation values greater than 2 are indicated in red; fold-change values less than 0.5 and fold-regulation values less than −2 are indicated in blue.

Table W3. β-Catenin Mutational Status in Hepatoblastoma Specimens.

Sample	Histology	Mutational Status	CITED1 Densitometry	β-Catenin Densitometry
1	2	2	40.73	1.15
2	1	2	28.97	1.28
3	2	ND	27.79	0.61
4	2	ND	40.36	0.56
5	1	1	39.13	0.2
6	2	2	19.84	0.4
7	1	1	31.18	0.63
8	1	2	7.14	0.34
9	2	1	52.66	0.56
10	1	1	ND	1.77
11	1	ND	40.27	1.42
12	2	2	43.9	1.47
13	2	2	63.69	1.02
14	2	ND	47.42	1.29
15	1	1	9.78	0.28
16	1	2	42.78	1.7
17	2	2	40.82	1.58
18	2	2	18.07	ND
19	2	2	41.59	0.42

Histology 1, fetal; histology 2, EMEF; mutational status 1, wild type; mutational status 2, mutant; ND, not determined.

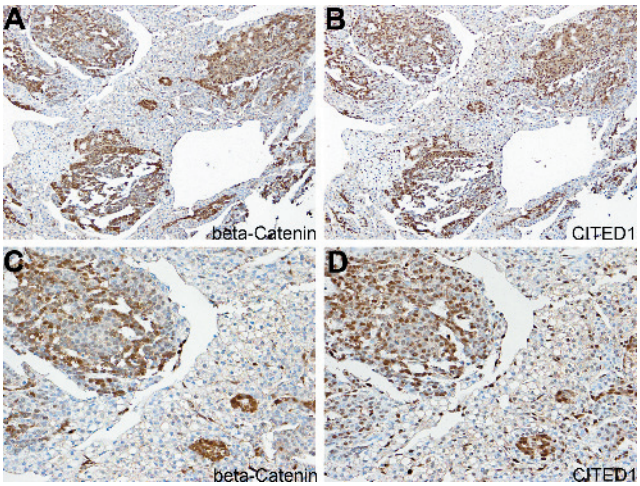

Figure W1. Serial sections immunohistochemically stained for β-catenin and CITED1 reveal expression in similar cell populations (serial sections A and B: original magnification, ×200; serial sections C and D: original magnification, ×400).